

G²Retro: Two-Step Graph Generative Models for Retrosynthesis Prediction

Ziqi Chen¹, Oluwatosin R. Ayinde², James R. Fuchs², Huan Sun^{1,3}, Xia Ning^{1,3,4} ✉

¹Computer Science and Engineering, The Ohio State University, Columbus, OH 43210. ²Medicinal Chemistry and Pharmacognosy, College of Pharmacy, The Ohio State University, Columbus, OH 43210. ³Translational Data Analytics Institute, The Ohio State University, Columbus, OH 43210. ⁴Biomedical Informatics, The Ohio State University, Columbus, OH 43210. ✉ning.104@osu.edu

Retrosynthesis is a procedure where a molecule is transformed into potential reactants and thus the synthesis routes are identified. We propose a novel generative framework, denoted as G²Retro, for one-step retrosynthesis prediction. G²Retro imitates the reversed logic of synthetic reactions, that is, first predicting the reaction centers to convert the target molecule into fragments named synthons, and then transforming synthons into reactants, following previous semi-template-based methods. In predicting reaction centers, G²Retro defines a comprehensive set of reaction center types, and enables diversity in the predicted reactions by considering multiple reaction center candidates. In completing synthons, G²Retro deploys a sequence of substructure attachments to transform synthons into reactants, which utilize a holistic view of the most updated structures of the synthons to be completed, as well as all the involved synthon and product structures. Here we show that G²Retro is able to better prioritize the most possible reactants in the benchmark dataset than the state-of-the-art methods, and discover novel and highly likely reactions that are not included in the benchmark dataset.

Drug development is time-consuming and costly: it takes approximately 10-15 years and \$1 to \$1.6 billion¹ to fully develop a new drug. One of the key steps in drug development is the identification of drug-like small molecules that display desired properties against a specific biomolecular target and then the synthesis of such molecules if they do not exist. Retrosynthesis is a procedure where such a desired molecule is transformed into potential reactants and thus the synthesis routes are identified. An extensive, diverse library of high-quality synthesis paths for a given molecule can enable more feasible reaction solutions starting from commercially available, building-block chemicals and provide more options for operationally simple, high yielding transformations using widely accessible reagents. The success and efficiency of retrosynthesis of drug-like small molecules immensely impact the entire drug development process and affect its success rate, costs, and speed.

Current retrosynthesis analysis is primarily conducted by synthetic and medicinal chemists based on their knowledge and experience, which could be limited or susceptible to human error. Consequently, the planned synthetic routes may not be diverse enough to cover novel, economic or green reactions. There exist proprietary synthesis reaction databases manually curated from the literature, including Reaxys² and SciFinder.³ Unfortunately, the high prices of these databases act to limit their accessibility in some academic and small biotech settings. Even with the aid of these databases, the development of new reactions and synthetic pathways for the preparation of challenging molecules remains non-trivial. In addition, database searches can be time-consuming with low throughput, particularly without extensive domain knowledge to guide the process. Recent *in silico* retrosynthesis prediction methods using deep learning⁴⁻⁷ have enabled alternative computationally generative processes to accelerate the conventional paradigm. These deep-learning methods learn from string-based representations (SMILES) or graph representations of given molecules, and generate possible reactant structures that can be used to synthesize these molecules, leveraging the advancement of natural language processing,⁸ graph neural networks,⁹ auto-encoders¹⁰ and other techniques in deep learning. They have demonstrated strong potential to significantly accelerate and advance retrosynthesis analysis. In this manuscript, we focus on the one-step retrosynthesis prediction, which predict the possible direct reactants for the synthesis of the target molecules, and act as the foundation of multi-step retrosynthesis analysis.¹¹

We propose a novel generative framework for one-step retrosynthesis prediction, denoted as G²Retro. G²Retro imitates the reversed logic of synthetic reactions: it first predicts the reaction centers in target molecules (denoted herein by “products”), identifies the fragments (denoted herein as “synthons”) needed to assemble the final products, and transforms these synthons into reactants, following a semi-template-based approach.^{5,7,12} In predicting reaction centers, G²Retro learns from the molecular graphs of the products and encodes their molecule structures most indicative of multiple reaction center types. G²Retro can also integrate fragment information in molecule structure learning; G²Retro with fragments is denoted as G²Retro-B. In completing synthons, G²Retro leverages the holistic view of all involved synthon and product structures, as well as their complementary relations, to identify the optimal completion actions. G²Retro allows multiple reaction centers and multiple completion paths for each product to increase diversity in its predictions. Meanwhile, to limit the exhaustive, full-scale generation of all possible reactions, G²Retro prioritizes the most possible ones via a new beam search strategy. Distinctly from existing retrosynthesis prediction methods that operate over molecule SMILES strings¹³⁻¹⁵ (i.e., template-free methods), G²Retro learns from molecular graphs that encode information most directly relevant to synthetic transformations. However, differently from existing methods using molecular graphs, G²Retro considers not only the structures of the synthons to be completed, but also the structures of other synthons from the

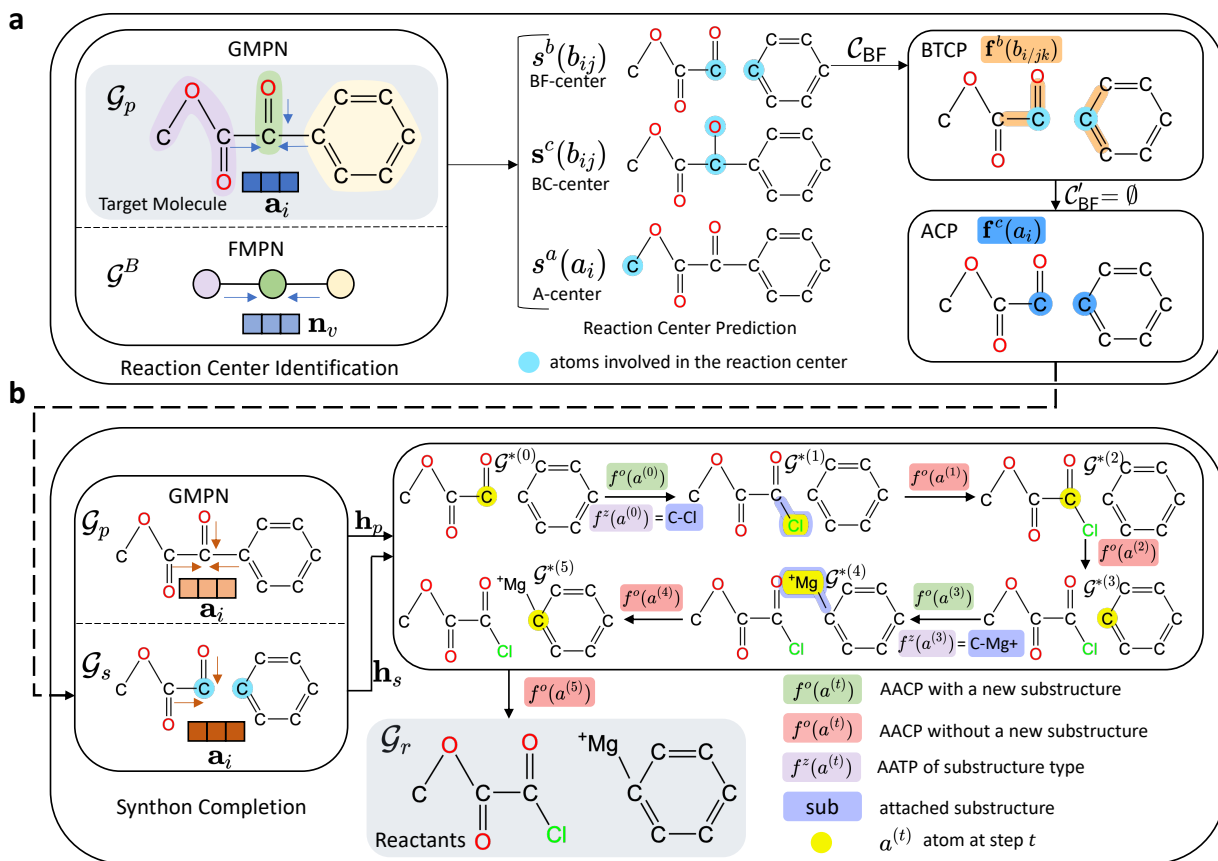


Fig. 1 | G²Retro retrosynthesis prediction process. **a**, G²Retro reaction center identification. G²Retro uses a graph message passing network (GMPN) and G²Retro-B uses additionally a fragment-graph message passing network (FMPN) to learn atom/fragment and bond embeddings; G²Retro predicts three types of reaction centers: newly formed bonds (BF-center), bonds with type changes (BC-center), and atoms with leaving fragments (A-center); for BF-center, G²Retro also predicts bonds that have type changes induced by the newly formed bonds (BTCP); for all the reaction center types, G²Retro predicts atoms with charge changes (ACP). **b**, G²Retro synthon completion. G²Retro uses GMPN to represent both the products and the synthons; G²Retro sequentially predicts whether a new substructure should be attached (AACP) and the type of the attachment (AATP); G²Retro adds predicted substructures until AACP predicts ‘stop’.

same products, so as to utilize their relations during reactions. In addition, G²Retro completes synthons by sequentially adding very small substructures instead of single atoms or bonds. Figure 1 presents an overview of G²Retro.

As a summary, G²Retro has the following advantages:

- G²Retro leverages a semi-template-based approach, predicts multiple types of reaction centers in products first, and converts the resulted synthons into reactants, best imitating the reversed logic of synthetic reactions, and enabling step-wise interpretability.
- G²Retro defines a comprehensive set of reaction center types, covering 97.5% of the test data and conforming to synthetic chemistry knowledge. Novel, customized deep neural networks are developed to predict each type of the reaction centers with high accuracies. Multiple reaction center candidates are considered for each product to enable diversity in the predicted reactions.
- G²Retro deploys a sequence of substructure (i.e., only bonds and rings) attachments to complete synthons into reactants, which utilize a holistic view of the most updated structures of the synthon to be completed, and the structures of the final product and other synthons.
- G²Retro operates over molecular graphs using new graph neural networks, better capturing the molecular structures that determine their synthesis feasibility and synthetic reactions.
- G²Retro employs a new, effective beam search strategy that prioritizes the most possible reactants along the synthon completion paths.
- G²Retro is compared with twenty baseline methods and demonstrates its state-of-the-art performance over the benchmark dataset. Case studies indicate that G²Retro could discover novel and highly likely reactions that are not included in the benchmark dataset.

Related Work

Deep-learning-based retrosynthesis prediction methods are typically categorized into three classes: template based (TB), template free (TF) and semi-template based (Semi-TB).

Template-based methods

Template-based methods formulate the retrosynthesis problem as a selection problem over a set of reaction templates. These templates can be either hand-crafted by experts¹⁶ or automatically extracted from known reactions in databases.^{4, 17–20}

Szymkuc *et al.*¹⁶ provided a review on using reaction templates coded by human experts for synthetic planning. However, these rules may not cover a large set of reactions due to the limitation of human annotation capacity. Recent template-based methods extract reaction templates automatically from databases. With the reaction templates available, Coley *et al.*¹⁷ (Retrosim) selected the reaction templates that the corresponding reactions in the database have the products most similar with the target molecules, in order to synthesize the target molecules. Dai *et al.*⁴ learned the joint probabilities of templates matched in the product molecules and all its possible reactants using two energy functions, one for reaction template scoring and the other for reactant scoring conditioned on templates. Seidl *et al.*¹⁹ (MHNreact) learned to associate the target molecule with the relevant reaction templates using a modern Hopfield network. Chen *et al.*²⁰ (LocalRetro) scored the suitability of all the reaction templates at all the potential reaction centers (atoms and bonds) in the target molecule. The use of templates provides interpretability towards the reasoning behind the generated reactions. However, these templates also limit the template-based methods to the reactions only covered by the templates.

Template-free methods

Template-free methods directly learn to transform the product into the reactants without using the reaction templates.^{6, 13–15, 21–25} Most template-free methods utilize the sequence representations of molecules (SMILES) and formulate the transformation between the product and its corresponding reactants as a sequence-to-sequence problem. Many SMILES-based methods use Transformer,⁸ a language model with attention mechanisms to model the relationship across tokens. Transformer follows the encoder-decoder architecture, which encodes the product SMILES string into a latent vector and then decodes the vector into the reactant SMILES strings. For example, Tetko *et al.*²⁴ (AT) learned to transform a product into its reactants using a Transformer trained on a dataset augmented with various non-canonical SMILES representations of each molecule. In AT, each target molecule was tested multiple times using different SMILES string representations. Kim *et al.*¹⁵ (TiedTransformer) learned the transformation from a product to its reactants using two coupled Transformers with shared parameters, one for the forward product prediction (synthesis) and the other for the backward reactant prediction (retrosynthesis). During the inference, they leveraged both the forward and backward models to find the best reactions. Sun *et al.*⁶ (Dual) transformed a product to its reactants using an energy-based framework. They also leveraged the duality of the forward and backward models by training them together and selected the best reactions with the highest energy value from the two models. Template-free methods are independent of reaction templates and thus have better generalizability to unknown reactions. However, template-free methods lack interpretability towards the reasoning behind their end-to-end predictions. SMILES-based template-free methods also suffer from the validity issue that the generated sequences may fail to follow the grammar of SMILES strings or violate chemical rules.¹³

Semi-template-based methods

Semi-template-based methods^{5, 7, 12, 26, 27} do not use reaction templates, or they do not directly transform a product into its reactants. Instead, most semi-template-based methods follow a two-step workflow utilizing atom-mappings: (1) identify the reaction centers and transform the product into synthons (intermediate molecules) using the reaction centers; (2) complete the synthons into the reactants. Shi *et al.*⁵ (G2G) first predicted reaction centers as bonds that can be used to split the product into the synthons, and then utilized a variational autoencoder to complete synthons into reactants by sequentially adding new bonds or new atoms. Somnath *et al.*⁷ (GraphRetro) predicted the bonds with changed bond types or the atoms with changed hydrogen count as the reaction centers, and then completed the synthons by selecting the pre-extracted subgraphs that realize the difference between synthons and reactants. Wang *et al.*²⁶ (RetroPrime) formulated the reaction center identification and synthon completion problems as two sequence-to-sequence problems (i.e., product to synthon, and synthon to reactant), and trained two Transformers for these problems, respectively. The prediction of reaction centers first in the above methods allows better interpretability towards the reasoning behind the generation process. The two-step workflow also empowers these methods to diversify their generated reactants by allowing multiple different reaction center predictions forwarded into their synthon completion step. Other semi-templated-based methods utilize the atom-mappings in a different way. For example, Sacha *et al.*²⁷ (MEGAN) formulated retrosynthesis as a graph editing process from a product to its reactants. These graph edits include the change in the atom properties or the bond types, or the addition of the new atoms or the benzene rings into the synthons.

G²Retro also identifies the reaction centers and then completes the synthons into the reactants in a sequential way as G2G does. However, G²Retro is fundamentally different from G2G. G²Retro can cover multiple types of reaction centers while G2G takes only the newly formed bonds as the reaction center, which leads to lower coverage of G2G on the dataset. During synthon completion, G²Retro attaches substructures (e.g., rings and bonds) instead of single atoms as in G2G, into synthons to simplify the completion process. In addition, G²Retro uses other synthons to complete a synthon, while G2G does not consider other systems. MEGAN also applies an action to add the benzene rings in synthon completion, but it cannot attach other complex ring substructures as what G²Retro does. In addition, MEGAN does not follow the two-step workflow, and thus G²Retro is also fundamentally different from MEGAN.

Problem Definition

We focus on the one-step retrosynthesis prediction problem, that is, given the target molecule (i.e., product), we identify a set of reactants that can be used to synthesize the molecule through one synthetic reaction. We decompose the retrosynthesis prediction problem into two subproblems, following semi-template-based approaches. (1) The first subproblem is to identify the reaction center from the target molecule. We define the reaction center as the single bond that is either newly formed or has the bond type changed, or the single atom with changed hydrogen count during the reaction. We also incorporate into the reaction center the bonds neighboring the reaction centers that have type changes induced by

Table 1 | USPTO-50K data statistics

Dataset		Statistics
# training reactions		40,008
# validation reactions		5,001
# test reactions		5,007
training reactions	average size of products	26.0
	average size of larger reactants	21.9
	average size of smaller reactants	9.0
	average number of reactants	1.7
validation reactions	average size of products	25.9
	average size of larger reactants	21.8
	average size of smaller reactants	9.1
	average number of reactants	1.7
test reactions	average size of products	25.9
	average size of larger reactants	21.7
	average size of smaller reactants	9.2
	average number of reactants	1.7

the newly formed bond, and the atoms with charge changes within the target molecule (more details in “Reaction Center Identification” Section). The reaction centers break the product molecules into synthons, which are defined as “hypothetical units within the target molecule that represent a potential starting reagent in the retrosynthesis of that target molecule”.²⁸ (2) The second subproblem in our method is to convert the synthons into the reactants. The reactants are considered correct if they are reported feasible in benchmark data, or they are considered reasonable based on domain knowledge. The reactions that are included in benchmark data are referred to as ground truth. Please note that while there is always one ground-truth reaction for each product in the benchmark data, there exist actually numerous feasible reactions for each product.

Materials

Data Preprocessing and Experimental Settings

We used the benchmark dataset provided by Yan *et al.*¹² This dataset, also referred to as USPTO-50K, contains 50K chemical reactions that are randomly sampled from a large dataset collected by Lowe²⁹ from US patents published between 1976 and September 2016. Each reaction in the large dataset is atom-mapped so that each atom in the product is uniquely mapped to an atom in the reactants. The 50K reactions in USPTO-50K are classified into 10 reaction types by Schneider *et al.*³⁰ (Table 4). To avoid the information leakage issue¹² (e.g., reaction center is given in both the training and test data), all the product SMILES strings in USPTO-50K are canonicalized. We used exactly the same training/validation/test data splits of USPTO-50K as in the previous methods,^{12,17} which contain 40K/5K/5K reactions, respectively. Table 1 presents the data statistics.

We train G²Retro models on the 40K training data, with parameters tuned on the 5K validation data, and test on the 5K test data. Following the prior work,^{4,5,7,17} we use the top- k ($k=1,3,5,10$) accuracy to evaluate the overall performance of all the methods. Top- k accuracy is the ratio of test products that have their ground truth correctly predicted among their top- k predictions. Higher top- k accuracy indicates better performance. Also following the prior work,⁷ we use the top- k accuracy ($k=1,2,3,5$) to evaluate the performance of reaction center identification and synthon completion.

Baseline Methods

We compared G²Retro with the state-of-the-art baseline methods for the one-step retrosynthesis problem, including five template-based (TB) methods, ten template-free (TF) methods and five semi-template-based (Semi-TB) methods.

Template-based baseline methods The five TB baseline methods include Retrosim, Neuralsym, GLN, MHNreact and LocalRetro. These methods first mine reaction templates from training data and apply only these templates to construct reactants from the target molecule.

- Retrosim¹⁷ selects the templates of reactions that produce molecules most similar to the target molecule.
- Neuralsym¹⁸ predicts suitable templates using product fingerprints through a multi-layer perceptron.
- GLN⁴ predicts reactions using two energy functions, one for template scoring and the other for reactant scoring conditioned on templates.
- MHNreact¹⁹ learns the associations between molecules and reaction templates using modern Hopfield networks, and selects templates based on the associations.
- LocalRetro²⁰ selects templates against each atom and each bond using classifiers.

Template-free baseline methods The ten TF baseline methods all use Transformer over SMILES string representations of products and/or reactants.

- SCROP¹³ maps the SMILES strings of products to the SMILES strings of reactants using a Transformer, and then corrects syntax errors (e.g., mismatch of parentheses in SMILES strings) to ensure valid reactant SMILES strings.
- LV-Trans¹⁴ pre-trains a vanilla Transformer using reactions generated from templates, and then fine-tunes the Transformer with a multinomial latent variable representing reaction types.
- GET²¹ trains standard Transformer encoders and decoders using the combined atom representations learned from molecular graphs and from SMILES strings.
- Chemformer²² translates product SMILES strings into reactant SMILES strings using Transformer, which is pre-trained on an independent dataset to recover masked SMILES strings (i.e., with some atoms masked out) or to normalize augmented SMILES strings (i.e., multiple, equivalent non-canonical SMILES strings for each SMILES string).
- Graph2SMILES²³ encodes molecular graphs using graph neural networks with attention mechanisms, and decodes the reactant SMILES strings from the graph representations using a Transformer decoder.
- TiedTransformer¹⁵ uses two Transformers with shared parameters to learn the transformation from products to reactants and vice versa, respectively, and selects the best reactions using the likelihood values from these two Transformers.
- GTA³¹ enhances a Transformer with truncated attention connections regulated by molecular graph structures.
- Dual⁶ uses an energy-based model with two Transformers to learn the transformation from product SMILES strings to reactants’ SMILES strings and vice versa, and selects the best reactions using the energy.
- AT²⁴ trains a Transformer using augmented product and reactant SMILES strings and predicts reactants also using augmented product strings.
- Retroformer²⁵ integrates a reaction center detection module within a Transformer, and decodes reactants utilizing the predicted reaction centers.

Semi-template-based methods The five Semi-TB baseline methods all use molecular graph representations. Most of them explicitly predict reaction centers first.

- RetroPrime²⁶ trains two Transformers independently to predict the transformation from the product to its synthons and from the synthons to the reactants, respectively.
- RetroXpert¹² predicts reaction centers on molecular graphs via a graph attention network, and transforms resulting synthons to reactants using a Transformer.
- G2G⁵ predicts reaction centers on molecular graphs via a graph neural network, and completes synthons into reactants through sequential additions of new atoms or bonds using the latent variables sampled from the latent space of a variational graph autoencoder.
- GraphRetro⁷ predicts reaction centers via a message passing neural network over molecular graphs, and completes synthons by selecting the subgraphs in a vocabulary that realize the difference between the synthons and reactants.
- MEGAN²⁷ transforms the product molecular graphs into the corresponding reactant graphs using a sequence of graph edits (e.g., change atom charges, add a new bond) that are learned from products and their reactants in the training set.

Experimental Results

Overall Comparison

Table 2 presents the overall comparison between G²Retro and the baseline methods on one-step retrosynthesis under two conditions, following the standard protocol in literature:^{4–7, 12, 17, 18, 21, 26, 27} (1) when the reaction type is given *a priori* for both model training and inference (i.e., “Reaction type known”); and (2) when the reaction type is always unknown (i.e., “Reaction type unknown”). When the reaction type is known, G²Retro uses a one-hot encoder as an additional feature for each atom in product molecules indicating the reaction type. Note that the top-*k* accuracies of all the baseline methods are identical to those reported in their original papers (issues related to fair comparison are discussed later). Table 4 lists all the reaction types in the benchmark dataset.

Comparison with semi-template-based (Semi-TB) methods

When the reaction type is known, compared to other Semi-TB methods, G²Retro achieves the best performance on top-3 (84.2%), top-5 (88.5%) and top-10 (91.7%) accuracies, corresponding to 2.7%, 1.1% and 0.1% improvement over those from the best baseline MEGAN (82.0%, 87.5% and 91.6%) on these three metrics. In terms of top-1 accuracy, G²Retro-B achieves the third-best performance (63.6%) compared to those of RetroPrime (64.8%) and GraphRetro (63.9%) on this metric. While G²Retro underperforms RetroPrime on one metric, it is significantly better than RetroPrime on all the other metrics: G²Retro outperforms RetroPrime on top-3 accuracy at 3.2%, on top-5 accuracy at 4.1%, and on top-10 accuracy at 5.6%.

When the reaction type is unknown, a similar trend is observed: G²Retro-B outperforms all the Semi-TB baseline methods on all the top accuracy metrics, with 0.7% improvement over the best baseline GraphRetro on top-1 accuracy, 4.7% improvement over the best baseline RetroPrime on top-3 accuracy, and 3.6% and 0.7% improvement over the best baseline MEGAN on top-5 and top-10 accuracies, respectively. G²Retro has a performance similar to that of G²Retro-B, with an even better top-3 performance 74.6% that is 5.4% improvement from that of RetroPrime.

Compared with the performance with known reaction types, all the methods including G²Retro and G²Retro-B have worse performance when the reaction types are unknown. It is well known in synthetic chemistry that there are several well-characterized reaction types (Table 4). These types have distinct patterns in their reactions and reaction centers. For example, acylation reactions are very common approaches to creating amide and sulfonamide linkages. They are known

Table 2 | Overall comparison in top- k accuracy (%)

Method type	Method	Reaction type known				Reaction type unknown			
		1	3	5	10	1	3	5	10
Template-based	Retrosim	52.9	73.8	81.2	88.1	37.3	54.7	63.3	74.1
	Neuralsym	55.3	76.0	81.4	85.1	44.4	65.3	72.4	78.9
	GLN	64.2	79.1	85.2	90.0	52.5	69.0	75.6	83.7
	MHNreact	-	-	-	-	50.5	73.9	81.0	87.9
	LocalRetro	63.9	86.8	92.4	96.3	53.4	77.5	85.9	92.4
Template-free	SCROP	59.0	74.8	78.1	81.1	43.7	60.0	65.2	68.7
	LV-Trans	-	-	-	-	40.5	65.1	72.8	79.4
	GET	57.4	71.3	74.8	77.4	44.9	58.8	62.4	65.9
	Chemformer	-	-	-	-	54.3	-	62.3	63.0
	Graph2SMILES	-	-	-	-	51.2	66.3	70.4	73.9
	TiedTransformer	-	-	-	-	47.1	67.1	73.1	76.3
	GTA	-	-	-	-	51.1	67.6	74.8	81.6
	Dual	65.7	81.9	84.7	85.9	53.6	70.7	74.6	77.0
	AT	-	-	-	-	53.2	-	80.5	85.2
	Retroformer	64.0	82.5	86.7	90.2	53.2	71.1	76.6	82.1
Semi-template based	RetroXpert	62.1	75.8	78.5	80.9	50.4	61.1	62.3	63.4
	G2G	61.0	81.3	86.0	88.7	48.9	67.6	72.5	75.5
	GraphRetro	63.9	81.5	85.2	88.1	53.7	68.3	72.2	75.5
	MEGAN	60.7	82.0	87.5	91.6	48.1	70.7	78.4	86.1
	RetroPrime	64.8	81.6	85.0	86.9	51.4	70.8	74.0	76.1
	G ² Retro	63.1	84.2	88.5	91.7	<u>53.9</u>	74.6	<u>80.7</u>	<u>86.6</u>
	G ² Retro-B	63.6	<u>83.6</u>	<u>88.4</u>	91.5	54.1	<u>74.1</u>	81.2	86.7

Columns with 1, 3, 5 and 10 present top-1, top-3, top-5 and top-10 accuracies, respectively. Best top- k accuracy values among the methods of each type are in **bold**. Top- k accuracy values of G²Retro and G²Retro-B are underlined if they are not the best but still better than all the baselines of the respective type.

for their efficiency and high yields, especially when they involve acyl/sulfonyl halides.³² The improved performance with known reaction types integrated into retrosynthesis model training demonstrates that leveraging *a priori* reaction type information could benefit retrosynthesis prediction in general. However, in real applications, reaction types are typically not available in retrosynthesis when only the target molecule is presented. The superior performance of G²Retro and G²Retro-B in “reaction type unknown” condition demonstrates their great utility in real applications.

Comparison with GraphRetro, MEGAN and RetroPrime GraphRetro, MEGAN and RetroPrime are three strong baselines. GraphRetro has good top-1 accuracies but much worse results on other top accuracy metrics. According to its authors,⁷ GraphRetro tends to bias its beam search to the most possible reaction center. Thus, it may prioritize the most possible reactants from the most possible reaction center at the very top of its predictions. However, if the most possible reaction centers are not the ground truth, GraphRetro would totally miss the ground truth in its beam search, resulting in poor performance on other top accuracy metrics. MEGAN has good top-10 accuracies, but consistently much worse top-1 accuracies than all the other methods. MEGAN edits the product graph into reactant graphs in a sequential manner. The poor performance on top-1 accuracy indicates that MEGAN’s sequential edits may not generalize well to test data; while MEGAN can still identify the ground-truth reactants, they are not predicted as the most likely. RetroPrime achieves the best top-1 accuracy with reaction type known. It uses augmented SMILES strings (i.e., each product has multiple, equivalent, non-canonical SMILES strings) in training the two sequence-to-sequence transformers. It is likely that top results in RetroPrime correspond to the ground truth but in different, augmented SMILES strings, and thus high top-1 accuracy but low and similar other top accuracies. These three Semi-TB baseline methods only perform well on one certain metric (in one certain condition), but do not show consistent optimality across many metrics or across the two conditions.

Compared to these baselines, G²Retro always achieves the best performance on all the top accuracy metrics (except on top-1 accuracy when reaction types are known). High top- k accuracies at all different k are desired as they indicate the holistically high ranking positions of the ground truth in the predicted reactions, and thus the capability of models in recovering knowledge from data. High top- k accuracies with $k > 1$ may signify novel yet plausible reactions, as will be examined later in Section “Case Study”. This is because high top- k ($k > 1$) accuracy implies that there might be a few reactions different from the ground truth but are very possible and thus are ranked on top. Such reactions may enable novel discoveries. From the above two aspects, over all the metrics, G²Retro and G²Retro-B achieve the overall best performance compared to the three strong Semi-TB methods.

Comparison between G²Retro and G²Retro-B G²Retro-B performs slightly better than G²Retro when the reaction types are unknown, but worse than G²Retro when the reaction types are known. G²Retro-B integrates synthetically accessible fragments in atom embeddings (Equation 6 in “Methods”). When the reaction types are unknown, the fragment

Table 3 | Module performance comparison in top-*k* accuracy (%)

Module	Method	Coverage (%)	Reaction type known				Reaction type unknown			
			1	2	3	5	1	2	3	5
Reaction center identification	G2G	97.9	90.2 (92.1)	94.5 (96.5)	94.9 (96.9)	95.0 (97.0)	75.8 (77.4)	83.9 (85.7)	85.3 (87.1)	85.6 (87.4)
	GraphRetro	95.0	84.6 (89.1)	92.2 (97.1)	93.7 (98.6)	94.5 (99.5)	70.8 (74.5)	85.1 (89.6)	89.5 (94.2)	92.7 (97.6)
	RetroPrime	100.0	84.6 (84.6)	94.0 (94.0)	96.7 (96.7)	97.9 (97.9)	65.6 (65.6)	81.3 (81.3)	87.7 (87.7)	92.0 (92.0)
	G ² Retro	97.5	84.3 (86.5)	94.6 (97.0)	96.5 (99.0)	97.0 (99.5)	69.5 (71.3)	85.6 (87.8)	90.8 (93.1)	94.8 (97.2)
	G ² Retro-B	97.5	85.0 (87.2)	94.1 (96.5)	96.2 (98.7)	97.3 (99.8)	69.3 (71.1)	85.4 (87.6)	91.1 (93.4)	94.7 (97.1)
Synthon completion	G2G	100.0	66.8	-	87.2	91.5	61.1	-	81.5	86.7
	GraphRetro	99.7	77.4 (77.6)	89.5 (89.8)	94.2 (94.5)	97.6 (97.9)	75.6 (75.8)	87.4 (87.7)	92.5 (92.8)	96.1 (96.4)
	RetroPrime	100.0	75.0	-	88.9	90.6	73.4	-	87.9	89.8
	G ² Retro	100.0	72.8	85.6	90.2	93.0	73.3	84.6	89.6	92.8

Columns represents: "Coverage(%)": the percentage of test reactions covered by the methods; 1, 3, 5 and 10: top-1, top-3, top-5 and top-10 accuracies; "(·)": the accuracy within the covered reactions; "-": not reported in literature.

information provides additional local contexts to atoms, which could facilitate better decisions on reaction center prediction and synthon completion. When the reaction types are known, atom embeddings directly integrate the reaction type information in G²Retro, which may outweigh the contextual information provided by the fragments, and thus G²Retro-B does not achieve additional performance improvement from G²Retro.

Comparison with template-free (TF) methods

G²Retro and G²Retro-B also demonstrate superior or competitive performance compared to TF methods on all the top accuracies. With reaction types known, G²Retro is the best on top-3, top-5 top-10 accuracies compared to all the template-free methods; with reaction types unknown, G²Retro-B is the best on top-3, top-5 and top-10 accuracies, and is the second best one on top-1 accuracy. For example, G²Retro is 4.9% better than the best TF method on top-3 accuracy (i.e., Retroformer) with the reaction types unknown. Most TF methods such as Dual and Chemformer have the competitive performance on top-1 accuracy but relatively worse results on other top accuracy metrics. This could be due to that TF methods with SMILES representations may fail to generate diverse or even many valid reactants with beam search,³³ leading to limited variation in their predicted results, and thus low and similar top-3, top-5 and top-10 accuracies. This lack of diversity and richness in the predictions, in addition to the lack of interpretability during the chemical sequence transformation process, could significantly hinder the application of TF methods in retrosynthesis prediction. To improve performance, AT tests each product molecule 100 times, each time with a different SMILES representation; it considers a correct prediction if any of the 100 tests predicts the ground truth. Thus, AT does a much more extensive exploration than other methods including G²Retro and G²Retro-B. Despite this, G²Retro outperforms AT on all the top accuracies with reaction types unknown. Compared to TF methods, G²Retro best imitates the reversed logic of synthetic reactions with two steps: reaction center identification and synthon completion, and overall, achieves better performance.

Comparison with template-based (TB) methods

G²Retro and G²Retro-B achieve competitive performance with that from the TB methods. With reaction types known, G²Retro achieves either the second or the third on all the top accuracies; with reaction types unknown, G²Retro-B achieves the best performance on top-1 (54.1%), and either the second or the third on all the other top accuracies. For example, with reaction types unknown, G²Retro-B is the second best on top-3 accuracy, with 3.8% difference from the best performance of LocalRetro; G²Retro-B slightly underperforms the second-best baseline MHNreact on top-10 (86.7% compared to 87.9% from MHNreact), but outperforms MHNreact on all the other metrics.

LocalRetro is a very strong TB method. It extracted 731 templates from the benchmark training data, whereas other TB methods have much more templates (11,647 for GLN and 9,162 for MHNreact). Therefore, LocalRetro could achieve better template selection over a small template set compared to others over much larger template sets. However, LocalRetro may suffer from scalability issues on large datasets because it scores all the reaction templates on all the potential reaction centers (i.e., all atoms and all bonds) in the product molecules. In general, all TB methods may not generalize well to novel reactions that are not covered by the templates.⁷ Unlike LocalRetro, G²Retro does not use reaction templates, and only scores all the bonds and atoms once for reaction center identification, and thus is much more scalable in inference. It learns the patterns from training data and thus has a better chance to discover new patterns from the training data that are not covered by templates.

Individual Module Performance

Following the typical evaluation for Semi-TB methods as in literature,⁷ Table 3 presents the performance of the two modules - reaction center identification and synthon completion in Semi-TB methods.

Comparison on reaction center identification

Among all the Semi-TB methods, the definitions of reaction centers vary. In G2G, reaction centers are referred to as the only one newly formed bond during the reaction, and reaction center identification predicts whether there is such a new bond (and its location) or not in the products as in a classification problem. This reaction center definition and

classification can cover 97.9% of the test data (the rest 2.1% correspond to multiple newly formed bonds). **GraphRetro** defines the reaction center as the newly formed bond (BF-center as defined in Section "Reaction Centers with New Bond Formation" but without induced bond changes), the changed bond (BC-center as in "Reaction Centers with Bond Type Change") and the single atom with changed hydrogen count (A-center as in "Reaction Centers with Single Atoms"), which in total covers 95.0% of the reactions in the test set. **RetroPrime** aims to identify all the atoms involved in the reactions as reaction centers, which covers all the reactions in the test set. **G²Retro** extends the definition of the reaction center in **GraphRetro** with induced bond type change and atom charge changes, covering 97.5% of the test set.

Due to the data leakage issue as revealed by Yan *et al.*¹² (i.e., reaction center is given in both the training and test data), the reported **G2G** reaction center identification performance as cited in Table 3 is overestimated¹. **GraphRetro** uses two functions, one for bonds and one for atoms, to predict reaction centers. While these functions are able to predict well when such bonds and atoms are truly reaction centers (i.e., performance in parentheses in Table 3), **GraphRetro**'s reaction center definition covers the least (95%) of the test set compared to the other methods, resulting in still low accuracies (i.e., performance outside parentheses) over the test set. **RetroPrime** has a very generic definition of reaction centers – any atoms involved in the reactions, and uses one unified model to predict these atoms. However, as these atoms may experience different changes (e.g., connected to or disconnected from other atoms), a unified model not customized to specific changes may not suffice, leading to overall relatively low accuracies compared to other methods, particularly when reaction types are unknown. **G²Retro** and **G²Retro-B** have the most comprehensive definition of reaction centers (Section "Reaction Center Identification") with high coverage (97.5%) on the test set. In addition, **G²Retro** and **G²Retro** use a specific predictor for each of the reaction center types. Therefore, they achieve the best overall accuracy among the entire test set, as well as good performance over the reactions covered by its reaction center definition.

Comparison on synthon completion

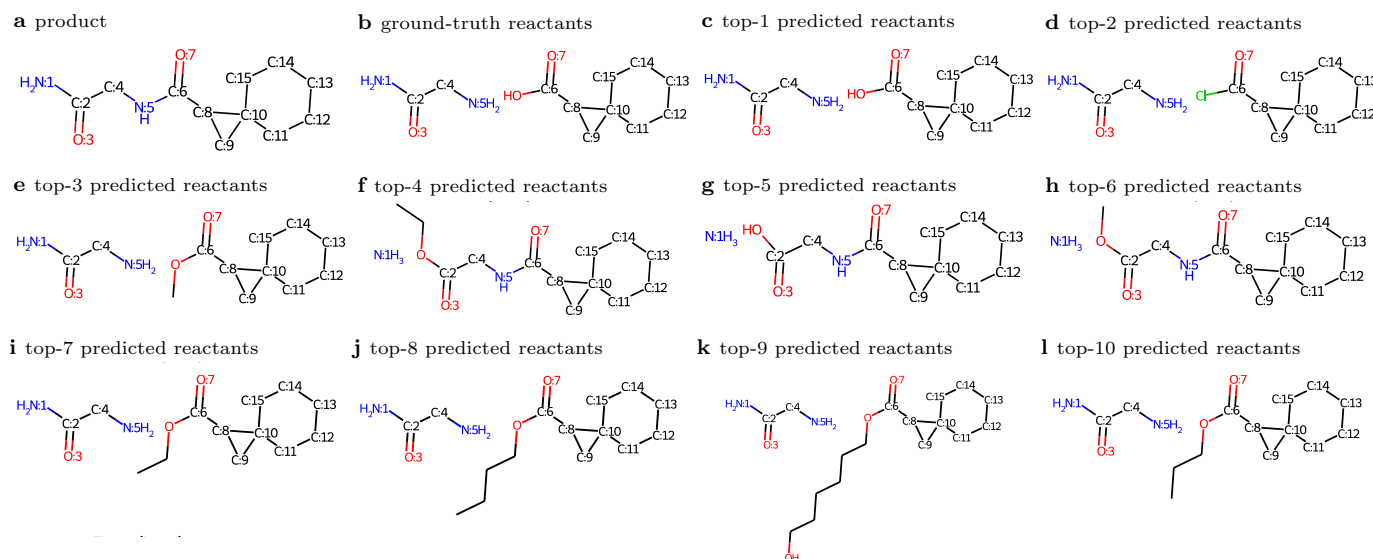
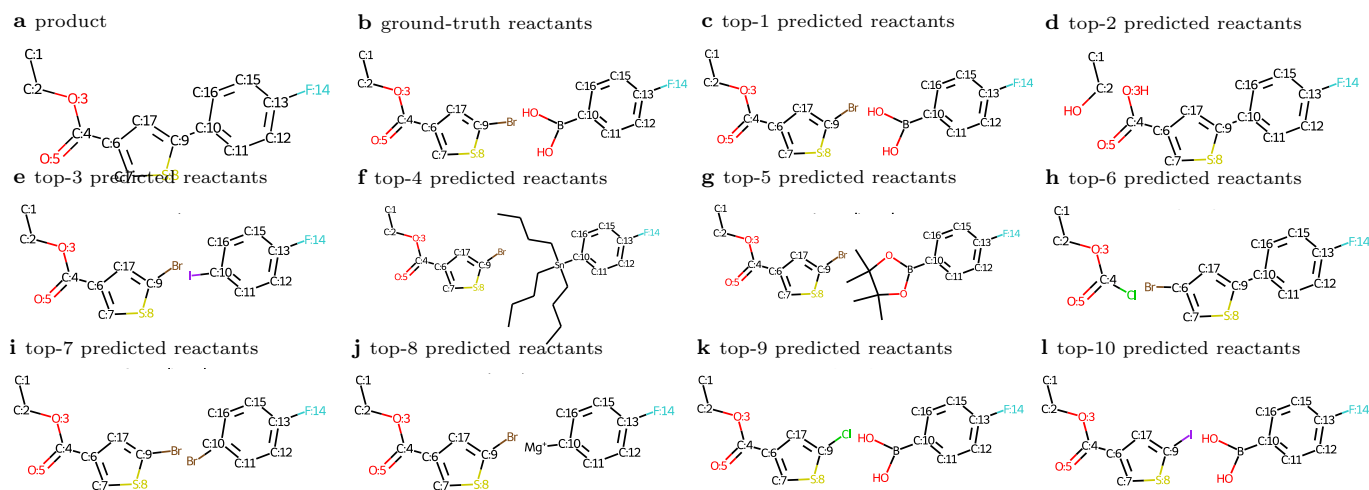
To compare synthon completion, all the reaction centers defined by different methods are given and used to start the completion processes. **G2G** predicts only bond establishment in its reaction center identification and thus has to deal with any associated changes such as bond type change in its synthon completion process, which complicates the synthon completion prediction. Therefore, its performance on synthon completion is the worst among all the methods. **GraphRetro** formulates the synthon completion as a classification problem over all the subgraphs that can realize the difference between the synthons and reactants. Therefore, its synthon completion is not guaranteed to work for all possible products (e.g., 99.7% coverage over the test set) if the needed subgraph is not included in the pre-defined vocabulary. Among all the products that **GraphRetro** can handle, its synthon completion performance is the best, due to that classification can be much easier than generation as all the other methods do. However, since **GraphRetro** does not do well in reaction center identification, overall, it does not outperform other methods in retrosynthesis prediction as Table 2 demonstrates. **RetroPrime** transforms the synthons to reactants using a Transformer, but similarly to **G2G**, also needs to deal with additional predictions such as bond type change. **RetroPrime**'s synthon completion performs reasonably well on top-1 accuracies. Together with its good top-1 accuracy on reaction center identification, **RetroPrime** achieves the best top-1 accuracy with reaction type known as demonstrated in Table 2. **G²Retro** does not use BRICS fragments in synthon completion because the fragment information is not available for the substructures that will be attached to synthons. Compared to **GraphRetro**, **G²Retro** leverages a generative process to add substructures to synthons in synthon completion, which is inherently more difficult than classification as in **GraphRetro**. On average, **G²Retro** outperforms **RetroPrime**, particularly on top-3 and top-5 accuracies. Combined with the strong performance on reaction center identification, the two modules together in **G²Retro** enable strong retrosynthesis prediction performance as in Table 2.

Performance on Different Reaction Types

Table 4 presents the top-*k* accuracy (*k*=1,3,5,10) of the reactions of different types. This method appears to predict certain reaction types more accurately than others as shown in Table 4. This is likely due to the relative structural diversity among potential reactants, particularly for substrates that can all provide the same products. For example, in the case of oxidations, only a very limited set of substrates can be utilized to generate a ketone, most commonly the oxidation of an alcohol, although ketones can certainly be accessed through other types of reactions as well. This leads to the relatively higher accuracies of **G²Retro** on the reactions of oxidations (e.g., 62.2% top-1 accuracy with reaction type unknown). In terms of reductions, however, numerous substrates could be utilized to generate an amine, including reductions of amides, nitro groups, and nitriles to name a few. In addition, there are numerous methods to access the same amines through various structurally unique deprotection reactions. The number of methods available to access a specific functional group, therefore, may make it more difficult to accurately predict which method has been used for a specific molecule, leading to the lower accuracies on reactions of deprotections (e.g., 58.3% top-1 accuracy with reaction type known). This would certainly be the case in carbon-carbon bond forming reactions as well, which can be assembled in a number of ways from various substrates, potentially leading to a somewhat lower prediction success rate (e.g., 37.2% top-1 accuracy with reaction type unknown). In addition, as shown in our case studies, in molecules containing more than one functional group, there are often multiple ways in which that molecule can be assembled by targeting each individual functional group as the reaction center. This means that there are multiple valid reaction pathways which could be considered by synthetic chemists in order to most efficiently construct a molecule.

Table 4 | G²Retro performance on different reaction types

Type Name	Percentage (%)	Reaction type known				Reaction type unknown			
		1	3	5	10	1	3	5	10
heteroatom alkylation and arylation	30.3	62.3	84.1	90.2	94.4	56.1	77.2	84.4	91.3
acylation and related processes	23.8	76.1	93.9	96.7	97.6	67.0	87.3	92.3	95.4
deprotections	16.5	58.3	87.2	91.5	93.9	51.8	76.5	82.7	87.9
C-C bond formation	11.3	48.1	68.1	75.7	82.4	37.2	56.6	67.9	75.7
reductions	9.2	72.5	87.9	91.8	95.0	52.7	69.8	78.1	84.6
functional group interconversion	3.7	50.5	69.0	75.5	81.0	42.4	52.7	60.9	67.9
heterocycle formation	1.8	-	-	-	-	-	-	-	-
oxidations	1.6	86.6	91.5	92.7	95.1	62.2	80.5	85.4	91.5
protections	1.4	85.3	89.7	89.7	89.7	48.5	67.6	85.3	86.8
functional group addition	0.5	95.7	95.7	95.7	95.7	78.3	82.6	87.0	87.0


Fig. 2 | Predicted reactions by G²Retro for product “NC(=O)CNC(=O)C1CC12CCCCC2”. Numbers next to each atom after the colon ‘:’ are the indices of the atoms. Atoms with same indices in different subfigures are corresponding to each other. **a**, product/target molecule; **b**, the ground-truth reactants in USPTO-50K; **c-l**, top predicted reactants.


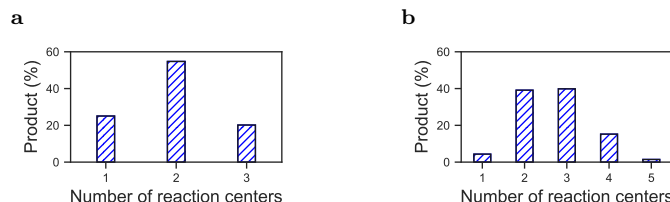


Fig. 4 | Distributions of products in terms of their predicted reaction centers. a, Products with hits at 3. b, Products with hits at 5.

of this molecule (Figure 2c). The other reactions predicted, however, are also very instructive into the strengths and limitations of G²Retro. In Figure 2a, the product has two amide groups in the side chain of the molecule. G²Retro identified both of these linkages as potential reaction centers (e.g., in Figure 2c between N:5 and C:6; in Figure 2g between N:1 and C:2). Typically, chemists would disconnect the molecule at the C:6 amide carbonyl rather than C:2 so that a fully elaborated side chain can be introduced to complete the molecule. This approach would generally be considered more efficient since its reaction introduces more complexity into the molecule in a single step and would therefore be predicted to limit the total number of steps necessary to construct the molecule. In some limited cases, however, it may be necessary to introduce the nitrogen at N:1 last (e.g., in Figure 2f-2h), so this should also be considered a feasible reaction. In addition to the typical amide coupling strategy, which takes place between an amine and a carboxylic acid, G²Retro also correctly identifies the reaction of the amine with an acid chloride to make the same bond (Figure 2d). Although this was not the strategy utilized in the ground-truth study, this strategy would certainly be expected to work in this case for construction of this molecule. The other common reaction that was predicted for this example was the nucleophilic addition of the N:5 (or N:1) amine into the C:6 (or C:2) carbonyl of an ester (N:5-C:6 - Figure 3e, 3i, 3j, 3k, 3l and N:1-C:2 - 3f and 3h). This type of reaction, which is essentially a transamidation reaction, should also work to provide the product. Interestingly, however, G²Retro predicts several different esters as substrates for this transformation (Figure 2c, 2e, 2i, 2j, 2k and 2l). While these are different substrates, the variation of the ester side chain in these cases would not be typically be considered as significantly different by a synthetic chemist unless steric or electronic contributions affect the reactivity/electrophilicity of the ester carbonyl.

Retrosynthesis of the product in Figure 3 involves a C-C bond forming reaction between C:9 and C:10 (Figure 3a). The disconnection of the carbon-carbon bond between the two aromatic rings, a heteroaromatic thiophene and a benzene ring in this case, represents the most obvious disconnection in the molecule. In this case, the top-1 reaction (Figure 3c) predicted by G²Retro for this transformation is a Suzuki coupling,³⁴ a common metal-mediated coupling between a boronic acid reactant and a corresponding aryl halide. This common transformation is the same reaction observed in the ground truth (Figure 3b). Interestingly, G²Retro also identifies additional permutations of this Suzuki reaction through changing the nature of the aryl halide (Figure 3k and 3l). Traditionally, aryl chlorides (Figure 3k) are less reactive than aryl bromides or iodides (Figure 3c and 3l) for coupling reactions and in the past were considered unreactive in these reactions. Newer methods³⁵ using specially designed ligands, however, have made the use of such chlorides possible. The other difference observed in the predicted Suzuki couplings is the use of a boronic ester (Figure 3g) versus a boronic acid (Figure 3c). Both boronic acids and boronic esters are common reagents for these transformations, with many being readily available from commercial sources. G²Retro also predicts that an esterification reaction at the C:4 carboxylic acid would also work to produce the desired compound (Figure 3d). While this is potentially not as synthetically useful for building the molecule, it is a reasonable transformation. Most impressively, G²Retro also predicts other coupling reactions³⁶ for the biaryl coupling reaction. These other methods include an Ullmann-type coupling³⁷ (Figure 3e and 3i), a Stille coupling³⁸ (Figure 3f), and a Kumada coupling^{35,39} (Figure 3j). This versatility predicted in the top-10 reactions may be of synthetic value for substrates if specific coupling methods fail or if the functionality necessary for one type of coupling reaction is not able to be easily prepared.

The above examples also demonstrate that G²Retro’s performance is underestimated by top-*k* accuracy alone, because its predicted reactions rather than the ground truth can still be possible and synthetically useful. Therefore, a more comprehensive evaluation strategy is needed not to miss those possible and potentially novel reactions. Discussions regarding *in vitro* validation are available in the “Discussions and Conclusions” section.

Diversity on predicted reactions

Diversity in predicted reactions is always desired, as it has the potential to enable novel discoveries on synthesis paths. G²Retro has the mechanisms to facilitate diverse predictions: The beam search strategy in G²Retro allows multiple reaction centers and multiple different attachments, and therefore potentially different scaffolds and structures in the predicted reactants. To analyze the diversity of G²Retro results, we identified a set of products such that their third or fifth predicted reactions are the ground truth, referred to as having a hit at 3 or 5, respectively. In this case, it is likely that their top-3 or top-5 predicted reactions are also possible. Figure 4 presents the distributions of these products in terms of different reaction centers among their top-3 and top-5 predicted reactions. Figure 4a shows that more than 50% of the products with a hit at 3 have their top-3 reactions from two different reaction centers; about 20% of the products have their top-3 reactions from three different reaction centers. Figure 4b shows that for products with a hit at 5, almost 40% have two reaction centers, and another 40% have three reaction centers, among their top-5 predicted reactions; more than 10% have four reaction centers. Thus, Figure 4 clearly demonstrates the diversity in terms of different reaction centers in G²Retro predictions.

Figure 5 presents an example of very diverse reactions predicted by G²Retro. For the product in Figure 5a, G²Retro

predicts three different reaction centers: an amide bond (between C:12 and N:11), a nitrogen-carbon bond (between N:7 and C:6) and ester (between O:3 and C:4). The patent reported that the target molecule was synthesized from a carboxylic acid derivative and an amine using amide coupling with a widely-used coupling reagent, EDC (Figure 5b). G²Retro predicted an acyl chloride-amine reactant pair as the top-1 result (Figure 5c), a potentially viable and even high yielding synthetic approach. It also predicts three reactant pairs from the other two reaction centers as possible routes within the top 4 (Figure 5d and 5f at which involve alkylation reactions to form the C:6-N:7 bond; Figure 5e at which forms the ester linkage between O:3 and C:4).

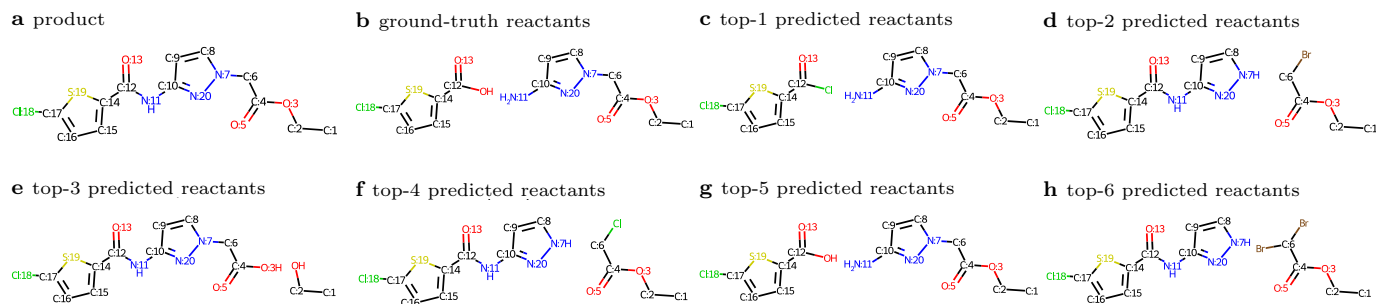


Fig. 5 | Predicted reactions by G²Retro for product “CCOC(=O)Cn1ccc(NC(=O)c2ccc(Cl)s2)n”. Numbers next to each atom after the colon ‘:’ are the indices of the atoms. Atoms with same indices in different subfigures are corresponding to each other. **a**, product/target molecule; **b**, the ground-truth reactants in USPTO-50K; **c-h**, top predicted reactants.

To further investigate the molecular similarities among the predicted reactants, we calculated reaction similarities. For two possible reactions of a product M_p , for example, $R_1: M_1 + M_2 \rightarrow M_p$ and $R_2: M_3 + M_4 \rightarrow M_p$, the similarity between these two reactions is calculated as follows:

$$\text{sim}(R_1, R_2) = \max(\text{sim}_m(M_1, M_3) + \text{sim}_m(M_2, M_4), \text{sim}_m(M_1, M_4) + \text{sim}_m(M_2, M_3)),$$

where $\text{sim}_m()$ is a similarity function over molecules. We used Tanimoto coefficient over 2,048-bit Morgan fingerprints as $\text{sim}_m()$. For each product, we calculated its all pairwise reaction similarities among all its top-10 reactions, and used the distribution of the reaction similarities to measure reaction diversity, that is, lower reaction similarities indicate higher reaction diversity. We clustered the products according to their reaction similarity distributions using the K-means clustering algorithm in Euclidean distances. Figure 6 presents the clustering results.

In Figure 6, the first four clusters have on average lower reaction similarities (on average 0.46 among the four clusters; 0.41, 0.45, 0.45, 0.49 in each of the clusters, respectively), and thus are referred to as high-reaction-diversity clusters (HRD); the other six clusters, referred to as low-reaction-diversity clusters (LRD), have relatively higher reaction similarities (on average 0.58 for among the six clusters; 0.52, 0.53, 0.58, 0.62, 0.67, 0.67 in each of the clusters, respectively). Figure 7 presents the distributions of reaction centers of these two clusters. Comparing Figure 7a and Figure 7b, HRD clusters tend to have more reaction centers than those in LRD, and the number of reaction centers correlates well with reaction diversity (-0.8486 between the average similarities and the number of reaction centers). Particularly, the first cluster, which has the highest reaction diversity (lowest reaction similarity), has on average 4.41 reaction centers, compared to the average 3.92 reaction centers of those in LRD clusters. The ninth and tenth clusters, which have the lowest reaction diversity, have on average 2.57 reaction centers. These results clearly show the diversity of G²Retro predictions.

Discussions and Conclusions

Comparison fairness among existing methods

In our study of the baseline methods, several issues were identified that introduce biases in method evaluation, and impede a fair comparison among many existing methods. In Table 2, RetroXpert’s results are from its updated GitHub,⁴⁰ as their results originally reported in their manuscript had a data leakage issue (all the reaction centers were implicitly given) and thus were overestimated.¹² G2G may also suffer from the data leakage issue as discussed,⁴¹ but G2G’s results were only available from its original paper, though likely overestimated. All the methods except Neursysm, LV-Trans, Dual and Retroformer published their code and datasets. Among these methods, most template-free methods including SCROP, GET, Chemformer, TiedTransformer, GTA and AT used the same data split, which is, however, different from the benchmark data split used in the other methods. For example, the training set of these template-free methods has 40,029 reactions, while the training set of the other methods including G²Retro has 40,008 reactions. Even though all the methods adopted the same ratio (i.e., 80%/10%/10% for training/validation/test set) to split the benchmark dataset, their splits, particularly their test sets, are not identical, leading to an unfair comparison among these methods. In this manuscript, we adopted the data split used by the previous semi-template based methods; for the template-free methods with different data splits, we still used the results reported by their authors.

Comparison among template-based, template-free and semi-template-based methods

Template-based methods were first developed for retrosynthesis prediction. They match products into pre-defined templates that are extracted from training data or hand-crafted based on knowledge. A notable advantage of templates is that they can enable strong interpretability (e.g., each template may correspond to a certain reaction type, a chemical scaffold, or a reactivity pattern) and thus result in reactions that better conform to domain knowledge. They can also well

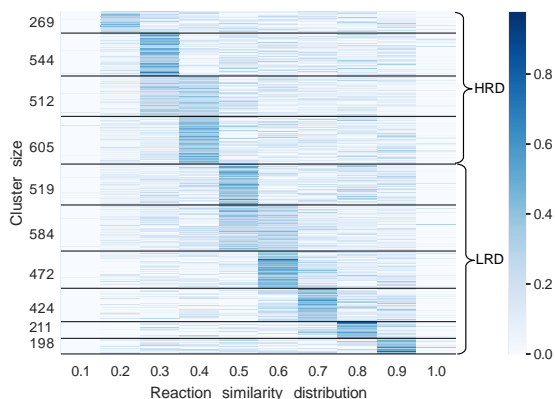


Fig. 6 | Clustering on test products based on predicted reaction diversities

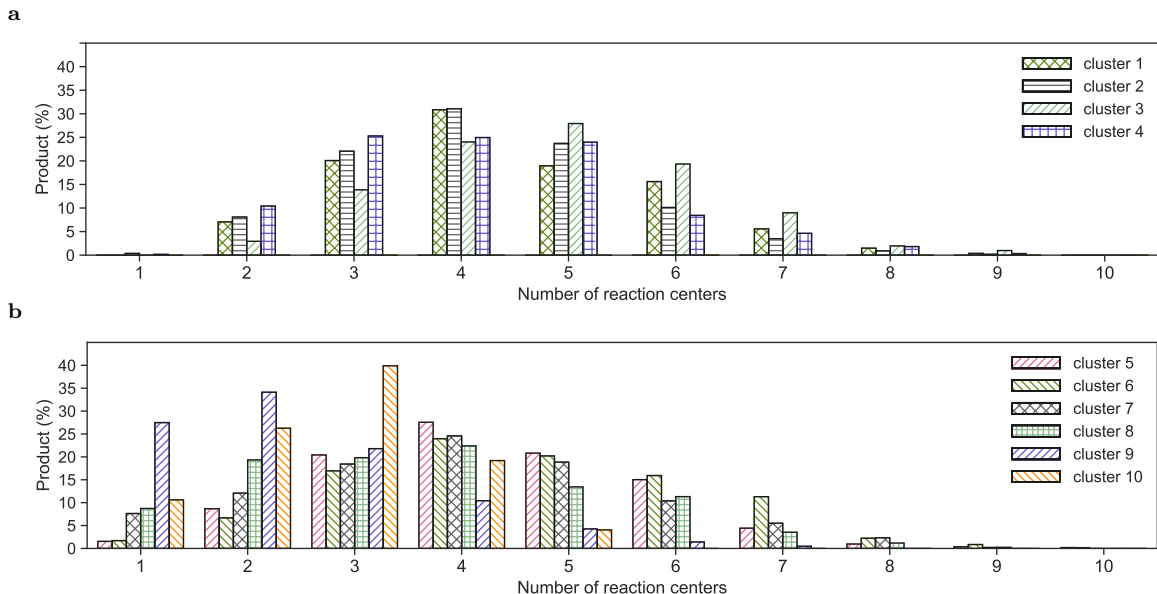


Fig. 7 | Test product distributions in terms of reaction diversities. **a**, Test product distributions among high-reaction-diversity clusters. **b**, Test product distributions among low-reaction-diversity clusters.

fit the data if the templates are extracted from the data. However, they suffer from a lack of strong learning capabilities and a lack of generalizability, if the templates do not cover and cannot automatically discover novel reaction patterns. In general, template-based methods underperform template-free and semi-template-based methods.

Template-free methods largely leverage the technological advancement in Natural Language Processing (NLP), including large-scale language models such as Transformer and BART, and also many pre-training techniques. They formulate a reaction as a SMILES string translation problem. Rather than enumerating pre-defined patterns (i.e., templates) as template-based methods do, template-free methods are equipped with much stronger learning capabilities from SMILES strings and can represent latent reaction transformation patterns in an operable manner. Although with improved performance compared to that of the template-based methods, unfortunately, template-free methods sacrifice their interpretability as it is non-retrieval to decipher why an atom (analogous to a token in NLP) is generated next along the SMILES strings, or what chemical knowledge the actions correspond to. In addition, as SMILES strings are a ‘flattened’ representation of molecular graphs according to the atom orderings from a graph traversal, template-free methods over SMILES strings cannot fully leverage molecular structures, which ultimately determine molecule synthesizability and reaction types.

Semi-template-based methods, typically over molecular graphs, represent the most recent and also in general the best performing retrosynthesis prediction methods. They utilize the most advanced graph representation learning paradigm to better capture molecule structures. They also take advantage of graph (variational) auto-encoder frameworks or sequential predictions to empower the models with generative ability. More importantly, semi-template-based methods can extrapolate to novel reactions using the latent representations learned from data. Meanwhile, semi-template-based methods usually explicitly predict reaction centers, better complying with how chemical reactions are understood. G^2 Retro is a semi-template-based method and achieves superior performance to other methods, demonstrating it as a state-of-the-art method for retrosynthesis prediction.

In vitro validation

The use of top- k accuracy as the evaluation metric has been dominating in the current retrosynthesis prediction research. However, as we have demonstrated in our case study, top- k accuracy has serious limitations and underestimates model performance. It only compares the predicted reactions with those in the benchmark data, but does not consider novel

predicted reactions that are not in the benchmark data but are highly likely. Such novel predictions should be assessed using existing data from very large reaction databases and evaluated from the perspective of a synthetic chemist, so to determine the accuracy and likelihood that these predicted approaches could be employed. Finally, the predicted reactions should be prioritized for synthesis and executed in the laboratory to determine whether or not they proceed as predicted. Such *in vitro* testing and validation are very much needed ultimately to truly translate the computational approaches into real impacts,

While no standard protocols for large-scale reaction validation exist, a funnel-shaped filtering protocol could be useful. First, high-throughput prioritization of the predicted reactions should be conducted to identify a feasible set of reactions for further validation, as the retrosynthesis prediction methods can easily produce many reactions, not feasible for manual investigation or selection. Forward synthesis prediction methods^{42,43} (i.e., predict products given reactants) trained from an independent dataset can be leveraged for quick prioritization. Such methods have been demonstrated to achieve good performance. Literature search (e.g., via SciFinder³ or Reaxys²) could follow to identify from the prioritized set those predicted reactions that match previously reported patterns of reactivity. Domain expertise in the area of chemical synthesis will be critical to selecting reactions based on the literature support and the commercial availability of their starting materials for a small-scale *in vitro* validation. All of the above represent challenging but interesting future research directions.

Conclusions

G²Retro predicts reactions of given target molecules by predicting their reaction centers, and then completing the resulting synthons by attaching small substructures. Based on a comparison against twenty baseline methods over a benchmark dataset, G²Retro achieves the state-of-the-art performance under most metrics. G²Retro also enables diverse predictions and novel reactions that were accessed as very possible by synthetic chemists. However, G²Retro still has several limitations. First, the three types of reaction centers in G²Retro still cannot cover all possible reaction center types (e.g., the reactions with multiple newly formed bonds). Therefore, a more comprehensive definition of reaction center types is still needed. G²Retro cannot cover bonds or rings that are attached at the reaction centers but do not appear in the training data either, as the substructures that G²Retro employs to complete synthons are extracted only from training data. In addition, the atom-mapping between products and reactants that is required by G²Retro (and required by many existing methods) to complete synthons is not always available or of high quality (it is available in USPTO-50K). To identify such mappings, it requires to calculate graph isomorphism, which is an NP-hard problem. Moreover, the sum of log-likelihoods of all the involved predictions (i.e., reaction center prediction, attached atom type prediction) that G²Retro uses to prioritize reactions, is not necessarily the same as the likelihood of the reactions, which could affect the quality of the prioritized reactions. We are also investigating a systemic evaluation and *in vitro* validation protocol, in addition to using top-*k* accuracy, as we discussed earlier. Multiple-step retrosynthesis could be possible by applying G²Retro multiple times iteratively, each time on a reactant as the target molecule. Connected after the deep generative models that have been developed to optimize small molecule structures and properties^{44,45} for lead optimization, G²Retro has a great potential to generate synthetic reactions for these *in silico* generated drug-like molecules, and thus substantially speed up the drug development process.

Methods

Following the prior semi-template-based methods,^{5,7} G²Retro generates reactants from products in two steps. In the first step, G²Retro identifies the reaction centers using the center identification module. The reaction center is defined as the atoms and the bonds that are changed during the reaction in order to synthesize the product. Given the reaction center, G²Retro converts the target molecule into a set of intermediate molecular structures referred to as synthons, which are incomplete molecules and will be completed into reactants. In the second step, G²Retro completes synthons into reactants by sequentially attaching bonds or rings in the synthon completion module. The intermediate molecular structures before being completed to reactants are referred to as updated synthons. Figure 1 presents the overall model architecture of G²Retro. All the algorithms are presented in Supplementary Section S2.

Molecule Representations and Notations

Table 5 presents the key notations used in this manuscript. A synthetic reaction involves a set of reactants $\{M_r\}$ and a product molecule M_p that is synthesized from the reactants². Each reactant M_r has a corresponding synthon M_s , representing the substructures of M_r that appear in M_p . We represent the product molecule M_p using a molecular graph \mathcal{G}_p^M , denoted as $\mathcal{G}_p^M = (\mathcal{A}, \mathcal{B})$, where \mathcal{A} is the set of atoms $\{a_i\}$ in M_p , and \mathcal{B} is the set of corresponding bonds $\{b_{ij}\}$, where b_{ij} connects atoms a_i and a_j . We also represent the set of the reactants $\{M_r\}$ or the set of synthons $\{M_s\}$ of M_p using only one molecular graph \mathcal{G}_r^M or \mathcal{G}_s^M , respectively. Here, \mathcal{G}_r^M and \mathcal{G}_s^M could be disconnected with each connected component representing one reactant or one synthon.

For synthon completion, we define a substructure z as a bond (i.e., $z = b_{ij}$) or a ring structure (i.e., $z = \{b_{ij}|a_i, a_j \in \text{a single or polycyclic ring}\}$) that is used to complete synthons into reactants. We construct a substructure vocabulary $\mathcal{Z} = \{z\}$ by comparing \mathcal{G}_r ’s and their corresponding \mathcal{G}_s ’s in the training data, and extracting all the possible substructures from their differences. In total, G²Retro extracted 83 substructures, covering all the reactions in the test data. Details about these substructures are available in Figure S1 in Supplementary Section S3. Note that different from templates

²We do not consider reagents or catalysts in this study.

Table 5 | Notations

Notation	Meaning
$M_r/M_s/M_p$	reactant/synthon/product molecule
$\mathcal{G} = (\mathcal{A}, \mathcal{B})$	molecular graph with atoms \mathcal{A} and bonds \mathcal{B}
a	an atom in \mathcal{G}
b_{ij}	a bond in \mathcal{G} connecting a_i and a_j
$\mathcal{G}^B = (\mathcal{V}, \mathcal{E})$	BRICS graph with BRICS fragments \mathcal{V} and edges \mathcal{E}
n	a BRICS fragment in \mathcal{G}^B
e_{uv}	an edge connecting two BRICS fragment
\mathbf{x}	a feature vector for an atom or a bond
\mathcal{C}_{BF}	a set of bonds neighboring the bond formation center
\mathcal{C}_A	a set of atoms within the reaction center
z	a substructure used to complete synthons into reactants
\mathcal{Z}	a vocabulary with all the substructures in the dataset

used in TB methods, the substructures G^2Retro used are only bonds and rings, and multiple bonds and rings can be attached to complete a synthon.

We also represent molecules using their fragments generated from the breaking retrosynthetically interesting chemical substructures (BRICS) fragmentation algorithm.⁴⁶ BRICS breaks synthetically accessible bonds in a product M_p , following a set of fragmentation rules. Thus, M_p can be represented as a BRICS graph $\mathcal{G}_p^B = (\mathcal{V}, \mathcal{E})$, where each node $n_u \in \mathcal{V}$ represents a BRICS fragment with all the atoms and bonds belonging to it, and each edge $e_{uv} \in \mathcal{E}$ corresponds to a bond b_{ij} that connects two BRICS fragments n_u and n_v (i.e., $a_i \in n_u$ and $a_j \in n_v$) (In our dataset, two BRICS fragments are connected through only one bond). Thus, \mathcal{E} include synthetically accessible bonds, which tend to be the reaction centers. Compared to \mathcal{G}_p^M , \mathcal{G}_p^B incorporates fragment-level structures of M_p . For simplicity, when no ambiguity arises, we omit the super/sub-scripts and use \mathcal{G} or \mathcal{G}^B to represent \mathcal{G}^M or \mathcal{G}_p^B , respectively.

Molecule Representation Learning

G^2Retro learns the atom representations over the molecular graph \mathcal{G} using the same message passing networks (MPN) as in Chen *et al.*⁴⁴ (algorithm A3 in Supplementary Section S2). For the product molecule M_p , G^2Retro also learns the representation for the BRICS fragments over the BRICS graph \mathcal{G}^B using the same MPN. G^2Retro with BRICS fragment learning is referred to as $\text{G}^2\text{Retro-B}$.

Atom Embedding over Molecular Graphs (GMPN)

G^2Retro first learns atom embeddings to capture the atom types and their local neighborhood structures by passing the messages along the bonds in the molecular graphs. Each bond b_{ij} is associated with two message vectors \mathbf{m}_{ij} and \mathbf{m}_{ji} . The message $\mathbf{m}_{ij}^{(t)}$ at t -th iteration encodes the messages passing from a_i to a_j , and is updated as follows,

$$\mathbf{m}_{ij}^{(t)} = W_1^a \text{ReLU}(W_2^a \mathbf{x}_i + W_3^a \mathbf{x}_{ij} + W_4^a \sum_{a_k \in \mathcal{N}(a_i) \setminus \{a_j\}} \mathbf{m}_{ki}^{(t-1)}), \quad (1)$$

where \mathbf{x}_i is the atom feature vector, including the atom type, valence, charge, the number of hydrogens, whether the atom is included in a ring and whether the ring is aromatic; \mathbf{x}_{ij} is the bond feature vector, including the bond type, whether the bond is conjugated or aromatic, and whether the bond is in a ring; W_i^a 's ($i=1,2,3,4$) are the learnable parameter matrices; $\mathbf{m}_{ij}^{(0)}$ is initialized with the zero vector; $\mathcal{N}(a_i)$ is the set with all the neighbors of a_i (i.e., atoms connected with a_i); and ReLU is the activation function. The message $\mathbf{m}_{ij}^{(t)}$ captures the structure of t -hop neighbors passing through the bond b_{ij} to a_j , by iteratively aggregating the neighborhood messages $\mathbf{m}_{ki}^{(t-1)}$. With the maximum t_a iterations, G^2Retro derives the atom embedding \mathbf{a}_i as follows,

$$\mathbf{a}_i = U_1^a \text{ReLU}(U_2^a \mathbf{x}_i + U_3^a \sum_{a_k \in \mathcal{N}(a_i)} \mathbf{m}_{ki}^{(1 \cdots t_a)}), \quad (2)$$

where $\mathbf{m}_{ki}^{(1 \cdots t_a)}$ denotes the concatenation of $\{\mathbf{m}_{ki}^{(t)} | t \in [1 : t_a]\}$; U_i^a 's ($i=1,2,3$) are the learnable parameter matrices. The embedding of the molecular graph \mathcal{G} is calculated by summing over all the atom embeddings as follows,

$$\mathbf{h} = \sum_{a_i \in \mathcal{G}} \mathbf{a}_i. \quad (3)$$

For M_p and M_s , their embeddings calculated from their molecular graphs as above are denoted as \mathbf{h}_p and \mathbf{h}_s , respectively.

BRICS Fragment Embedding over BRICS Graphs (FMPN)

$\text{G}^2\text{Retro-B}$ generates BRICS fragment embeddings by passing the messages along the connections over BRICS fragments in the BRICS graphs, in a similar way as for atom embeddings over molecular graphs. Specifically, each edge e_{uv} in \mathcal{G}^B

is associated with two message vectors \mathbf{e}_{uv} and \mathbf{e}_{vu} . The message $\mathbf{e}_{uv}^{(t)}$ at t -th iteration is updated as follows,

$$\mathbf{e}_{uv}^{(t)} = W_1^e \text{ReLU}(W_2^e \mathbf{s}_u + W_3^e \mathbf{s}_{uv} + W_4^e \sum_{n_w \in \mathcal{N}(n_u) \setminus \{n_v\}} \mathbf{e}_{wu}^{(t-1)}), \quad (4)$$

where $\mathbf{s}_u = \sum_{a_i \in n_u} \mathbf{a}_i$ aggregates the embeddings of all the atoms within the fragment n_u ; $\mathbf{s}_{uv} = \mathbf{a}_i$ is the embedding of atom a_i in n_u that is included in the edge e_{uv} ; W_i^e 's ($i=1,2,3,4$) are the learnable parameter matrices; $\mathbf{e}_{uv}^{(0)}$ is initialized with the zero vector. The message $\mathbf{e}_{uv}^{(t)}$ encodes the information passing through the edge e_{uv} to n_v , and thus is used to further derive the embedding of n_v as follows,

$$\mathbf{n}_v = U_1^e \text{ReLU}(U_2^e \mathbf{s}_v + U_3^e \sum_{n_w \in \mathcal{N}(n_v)} \mathbf{e}_{vw}^{(1 \cdots t_e)}), \quad (5)$$

where $\mathbf{e}_{vw}^{(1 \cdots t_e)}$ denotes the concatenation of $\{\mathbf{e}_{vw}^{(t)} | t \in [1 : t_e]\}$; U_i^e 's ($i=1,2,3$) are the learnable parameter matrices. With \mathcal{G}^B , G²Retro-B enriches the representation of atom a_i with the embedding \mathbf{n}_v of the fragment that a_i belongs to. Note that in BRICS algorithm, each atom only belongs to one fragment. The enriched atom representation is calculated as follows,

$$\mathbf{a}'_i = V(\mathbf{a}_i \oplus \mathbf{n}_v), \quad (6)$$

where V is a learnable hyperparameter matrix; \oplus represents the concatenation operation.

Reaction Center Identification (RCI)

Given a product M_p , G²Retro defines three types of reaction centers in M_p (algorithm A2 in Supplementary Section S2):

1. a new bond b_{ij} , referred to as bond formation center (BF-center), that is formed across the reactants during the reaction but does not exist in any of the reactants;
2. an existing bond b_{ij} in a reactant, referred to as bond type change center (BC-center), whose type changes during the reaction due to the gain or loss of hydrogens, while no other changes (e.g., new bond formation) happen; and
3. an atom in a reactant, referred to as atom reaction center (A-center), from which a fragment is removed during the reaction, without new bond formation or bond type changes.

The above three types of reaction centers cover 97.7% of the training set. The remaining 2.3% of the reactions in the training data involve multiple new bond formations or bond type changes, and will be left for future research. Note that with a single atom as the reaction center, the synthon is the product itself. We refer to all the transformations needed to change a product to synthons as product-synthon transformations, denoted as $p2s$ -T (algorithm A4 in Supplementary Section S2).

Reaction Centers with New Bond Formation (BF-center)

BF-center Reaction Center Prediction Following Somnath *et al.*,⁷ G²Retro derives the bond representations as follows,

$$\mathbf{b}_{ij} = U_1^b \text{ReLU}(U_2^b \mathbf{x}_{ij} + U_3^b (\mathbf{a}_i + \mathbf{a}_j) + U_4^b \text{Abs}(\mathbf{a}_i - \mathbf{a}_j)), \quad (7)$$

where $\text{Abs}(\cdot)$ represents the absolute difference; U_i^b 's ($i=1,2,3,4$) are the learnable parameter matrices. G²Retro uses the sum and the absolute difference of embeddings of the connected atoms to capture the local neighborhood structure of bond b_{ij} . Meanwhile, the two terms are both permutation-invariant to the order of \mathbf{a}_i and \mathbf{a}_j , and together can differentiate the information in \mathbf{a}_i and \mathbf{a}_j . In the case of G²Retro-B, the bond representations are derived by replacing the atom embeddings \mathbf{a}_i and \mathbf{a}_j with the enriched atom representations \mathbf{a}'_i and \mathbf{a}'_j calculated as in the Equation 6. With the bond representation, G²Retro calculates a score for each bond b_{ij} as follows,

$$s^b(b_{ij}) = \mathbf{q}^b \text{ReLU}(Q_1^b \mathbf{b}_{ij} + Q_2^b \mathbf{h}_p), \quad (8)$$

where \mathbf{h}_p is the representation of the product graph \mathcal{G}_p calculated as in Equation 3; \mathbf{q}^b is a learnable parameter vector and Q_1^b and Q_2^b are the learnable parameter matrices. G²Retro measures how likely bond b_{ij} is a BF-center using $s^b(b_{ij})$ by looking at the bond itself (i.e., \mathbf{b}_{ij}) and the structure of the entire product graph (i.e., \mathbf{h}_p). G²Retro scores each bond in M_p and selects the most possible BF-center candidates $\{b_{ij}\}$ with the highest scores. G²Retro breaks each product at each possible BF-center into synthons, and thus can generate multiple possible reactions.

BF-center Induced Bond Type Change Prediction (BTCP) In synthetic reactions, the formation of new bonds could induce the changes of neighbor bonds. Therefore, G²Retro also predicts whether the types of bonds neighboring the BF-center are changed during the reaction. Given the BF-center b_{ij} , the set of the bonds neighboring b_{ij} is referred to as the BF-center neighbor bonds, denoted as \mathcal{C}_{BF} , that is:

$$\mathcal{C}_{\text{BF}}(b_{ij}) = \{b_{ik} | a_k \in \mathcal{N}(a_i) \setminus \{a_j\}\} \cup \{b_{jk} | a_k \in \mathcal{N}(a_j) \setminus \{a_i\}\}. \quad (9)$$

Thus, G²Retro predicts a probability distribution $\mathbf{f}^b \in \mathbb{R}^{1 \times 4}$ for each neighboring bond in \mathcal{C}_{BF} , denoted as $b_{i/jk} \in \mathcal{C}_{\text{BF}}$, as follows,

$$\mathbf{f}^b(b_{i/jk}) = \text{softmax}(V_1^b \mathbf{b}_{i/jk} + V_2^b \mathbf{b}_{ij} + V_3^b \mathbf{h}_p), \quad (10)$$

where V_i^b 's ($i=1,2,3$) are the learnable parameter matrices. The first element \mathbf{f}_1^b in \mathbf{f}^b represents how likely the $b_{i/jk}$ type is changed during the reaction (It is determined as type change if \mathbf{f}_1^b is not the maximum in \mathbf{f}^b), and the other three represent how likely the original $b_{i/jk}$ in the reactant is single, double or triple bond, respectively (these three elements are reset to 0 if $b_{i/jk}$ type is predicted unchanged). Here, G^2Retro measures neighbor bond type change by looking at the neighbor bond itself (i.e., $\mathbf{b}_{i/jk}$), the BF-center (i.e., \mathbf{b}_{ij}) and the overall product (i.e., \mathbf{h}_p). G^2Retro updates the synthons \mathcal{G}_s by changing the neighboring bonds of the BF-center to their predicted original types. The predicted changed neighbor bonds are denoted as \mathcal{C}_{BF}' .

Reaction Centers with Bond Type Change (BC-center)

If a reaction center is due to a bond type change without new bond formations, G^2Retro calculates a score vector $\mathbf{s}^c \in \mathbb{R}^{1 \times 3}$ for each bond b_{ij} in M_p as follows,

$$\mathbf{s}^c(b_{ij}) = Q_1^c \text{ReLU}(Q_2^c \mathbf{b}_{ij} + Q_3^c \mathbf{h}_p), \quad (11)$$

where Q_i^c 's ($i=1,2,3$) are the learnable parameter matrices. Each element in $\mathbf{s}^c(b_{ij})$, denoted as $s_k^c(b_{ij})$ ($k = 1, 2, 3$), represents, if b_{ij} is the BC-center, the score of b_{ij} 's original type in \mathcal{G}_r being single, double, and triple bond, respectively. The element in \mathbf{s}^c corresponding to b_{ij} 's type in \mathcal{G}_p is reset to 0 (i.e., b_{ij} 's type has to be different in \mathcal{G}_r compared to that in \mathcal{G}_p). Thus, the most possible BC-center candidates $\{b_{ij}\}$ and their possible original bond types scored by $\mathbf{s}^c(\cdot)$ are selected. G^2Retro then changes the corresponding bond type to construct the synthons.

Reaction Centers with Single Atoms (A-center)

If a reaction center is only at a single atom with a fragment removed, G^2Retro predicts a center score for each atom a_i in M_p as follows,

$$s^a(a_i) = \mathbf{q}^a \text{ReLU}(Q_1^a \mathbf{a}_i + Q_2^a \mathbf{h}_p), \quad (12)$$

where \mathbf{q}^a is a learnable parameter vector and Q_1^a and Q_2^a are the learnable parameter matrices. G^2Retro selects the atoms $\{a_i\}$ in M_p with the highest scores as potential A-center's. In synthon completion, new fragments will be attached at the atom reaction centers.

Atom Charge Prediction (ACP)

Reaction Type Representation For all the atoms a_i involved in the reaction center or BF-center changed neighbor bonds \mathcal{C}_{BF}' , G^2Retro also predicts whether the charge of a_i remains unchanged in reactants. G^2Retro uses an embedding \mathbf{c} to represent all the involved bond formations and changes in $p2s\text{-T}$. If the reaction center is predicted as a BF-center at b_{ij} , G^2Retro calculates the embedding \mathbf{c} as follows,

$$\mathbf{c} = \sum_{b_{kl} \in \mathcal{C}_{\text{BF}}'(b_{ij}) \cup \{b_{ij}\}} W_1^c \text{ReLU}(W_2^c \mathbf{x}'_{kl} + W_3^c \mathbf{b}_{kl}), \quad (13)$$

where \mathcal{C}_{BF}' is a subset of \mathcal{C}_{BF} with all the bonds that changed types; \mathbf{x}'_{kl} is a 1×4 one-hot vector, in which $\mathbf{x}'_{kl}(0) = 1$ if bond b_{kl} is the bond formation center (i.e., $b_{kl} = b_{ij}$), or $\mathbf{x}'_{kl}(i) = 1$ ($i=1, 2, 3$) if b_{kl} type is changed from single, double or triple bond in reactants, respectively, during the reaction (i.e., b_{kl} is in $\mathcal{C}_{\text{BF}}'(b_{ij})$); W_i^c 's ($i = 1, 2, 3$) are the learnable parameter matrices.

If the reaction center is predicted as a BC-center at b_{ij} , \mathbf{c} is calculated as follows,

$$\mathbf{c} = W_1^c \text{ReLU}(W_2^c \mathbf{x}'_{ij} + W_3^c \mathbf{b}_{ij}), \quad (14)$$

where $\mathbf{x}'_{ij}(0) = 0$ and $\mathbf{x}'_{ij}(i) = 1$ ($i=1, 2, 3$) if b_{kl} type is changed from single, double or triple bond in reactants, respectively, during the reaction. If the reaction center is an A-center, no $p2s\text{-T}$ are needed and thus $\mathbf{c} = \mathbf{0}$.

Electron Change Prediction With the embedding \mathbf{c} for $p2s\text{-T}$, G^2Retro calculates the probabilities that a_i will have charge changes during the reaction as follows,

$$\mathbf{f}^c(a_i) = \text{softmax}(V_1^c \mathbf{a}_i + V_2^c \mathbf{c}), \quad (15)$$

where V_1^c and V_2^c are the learnable parameter matrices; $\mathbf{f}^c \in \mathbb{R}^{1 \times 3}$ is a vector representing the probabilities of accepting one electron, donating one electron or no electron change during the reaction. The option corresponding to the maximum value in \mathbf{f}^c is selected and will be applied to update synthon charges accordingly. G^2Retro considers at most one electron change since this is the case for all the reactions in the benchmark data.

Reaction Center Identification Module Training (RCI-T)

With the scores for three types of reaction centers, G^2Retro minimizes the following cross entropy loss to learn the above scoring functions (i.e., Equation 8, 11 and 12),

$$\mathcal{L}^s = - \sum_{b_{ij} \in \mathcal{B}} \left(y_{ij}^b l^b(b_{ij}) + \sum_{k=1}^3 \mathbb{I}_k(y_{ij}^c) l^c(b_{ij}) \right) - \sum_{a_i \in \mathcal{A}} y_i^a l^a(a_i), \quad (16)$$

where y^* ($x = a, b, c$) is the label indicating whether the corresponding candidate is the ground-truth reaction center of type $*$ ($y^* = 1$) or not ($y^* = 0$); $\mathbb{I}_k(x)$ is an indicator function ($\mathbb{I}_k(x) = 1$ if $x = k$, 0 otherwise), and thus $\mathbb{I}_k(y_{ij}^c)$

indicates whether the ground-truth bond type of b_{ij} is k or not ($k=1, 2, 3$ indicating single, double or triple bond); and $l^*(\cdot)$ ($* = a, b$)/($l_k^c(\cdot)$) is the probability calculated by normalizing the score $s^*(\cdot)/s_k^c$, that is, $l^*(x) = \exp(s^*(x))/\Delta$, where $\Delta = \sum_{b_{ij} \in \mathcal{B}} (\exp(s^b(b_{ij})) + \sum_{k=1}^3 \exp(s_k^c(b_{ij}))) + \sum_{a_i \in \mathcal{A}} \exp(s^a(a_i))$ ($l_k^c(x) = \exp(s_k^c(x))/\Delta$). Similarly, G²Retro also learns the predictor $\mathbf{f}^b(\cdot)$ for neighbor bond changes (Equation 10) and $\mathbf{f}^c(\cdot)$ for atom charge changes (Equation 15) by minimizing their respective cross entropy loss \mathcal{L}^b and \mathcal{L}^c . Therefore, the center identification module learns the predictors by solving the following optimization problem:

$$\min_{\Theta} \mathcal{L}^s + \mathcal{L}^b + \mathcal{L}^c, \quad (17)$$

where Θ is the set of all the parameters in the prediction functions. We used Adam algorithm to solve the optimization problem and do the same for the other training objectives.

Synthon Completion (SC)

Once the reaction centers are identified and all the product-synthon transformations (*p2s-T*) are conducted to generate synthons from products, G²Retro completes the synthons into the reactants by sequentially attaching substructures (algorithm A5 in Supplementary Section S2). All the actions involved in this process are referred to as synthon-reactant transformations (*s2r-T*). During the completion process, any intermediate molecules $\{M^*\}$ are represented as molecular graph $\{\mathcal{G}^*\}$. At step t , we denote the atom in the intermediate molecular graph $\mathcal{G}^{*(t)}$ ($\mathcal{G}^{*(0)} = \mathcal{G}_s$) that new substructures will be attached to as $a^{(t)}$, and denote the substructure attached to $a^{(t)}$ as $z^{(t)}$, resulting in $\mathcal{G}^{*(t+1)}$.

Atom Attachment Prediction (AAP)

The AAP algorithm is presented in algorithm A7 in Supplementary Section S2.

Attachment Continuity Prediction (AACP) G²Retro first predicts whether further attachment should be added to $a^{(t)}$ or should stop at $a^{(t)}$, with the probability calculated as follows,

$$f^o(a^{(t)}) = \sigma(V_1^o \mathbf{a}^{(t)} + V_2^o \mathbf{h}_s + V_3^o \mathbf{h}_p), \quad (18)$$

where

$$\mathbf{h}_s = \sum_{a_i \in \mathcal{G}_s} \mathbf{a}_i. \quad (19)$$

In Equation 18, $\mathbf{a}^{(t)}$ is the embedding of $a^{(t)}$ calculated over the graph $\mathcal{G}^{*(t)}$ (Equation 2); \mathbf{h}_s is the representation for all the synthons as in Equation 19; V_i^o 's ($i=1,2,3$) are the learnable parameter matrices; σ is the sigmoid function. In Equation 19, G²Retro calculates the representations by applying MPN over the graph \mathcal{G}_s that could be disconnected, and the resulted representation is equivalent to applying MPN over each \mathcal{G}_s 's connected component independently and then summing over their representations. G²Retro intuitively measures "how likely" the atom has a new substructure attached to it by looking at the atom itself (i.e., $\mathbf{a}^{(t)}$), all the synthons (i.e., \mathbf{h}_s), and the product (i.e., \mathbf{h}_p). Note that in Equation 18, BRICS fragment information (i.e., \mathbf{a}' as in Equation 6) is not used because the fragments for the substructures that will be attached to $a^{(t)}$ will not be available until the substructures are determined.

Attachment Type Prediction (AATP) If $a^{(t)}$ is predicted to attach with a new substructure, G²Retro predicts the type of the new substructure, with the probabilities of all the substructure types in the vocabulary \mathcal{Z} , calculated as follows,

$$\mathbf{f}^z(a^{(t)}) = \text{softmax}(V_1^z \mathbf{a}^{(t)} + V_2^z \mathbf{h}_s + V_3^z \mathbf{h}_p), \quad (20)$$

where V_i^z 's ($i=1,2,3$) are the learnable parameter matrices. Higher probability for a substructure type z indicates that z is more likely to be selected as $z^{(t)}$. The atoms $a \in z^{(t)}$ in the attached substructure are stored for further attachment, that is, they, together with any newly added atoms along the iterative process, will become $a^{(T)}$ ($T = t + 1, t + 2, \dots$) in a depth-first order in the retrospective reactant graphs. G²Retro stops the entire synthon completion process after all the atoms in the reaction centers and the newly added atoms are predicted to have no more substructures to be attached.

Synthon Completion Model Training (SC-T)

G²Retro trains the synthon completion module using the teacher forcing strategy, and attaches the ground-truth fragments instead of the prediction results to the intermediate molecules during training. G²Retro learns the predictors $f^o(\cdot)$ (Equation 18) and $\mathbf{f}^z(\cdot)$ (Equation 20) by minimizing their cross entropy losses \mathcal{L}^o and \mathcal{L}^z as follows:

$$\min_{\Phi} \mathcal{L}^o + \mathcal{L}^z, \quad (21)$$

where Φ is the set of parameters.

Inference

The algorithm for G²Retro inference is presented in algorithm A1 in Supplementary Section S2.

Top- K Reaction Center Selection

During the inference, G²Retro generates a ranked list of candidate reactant graphs $\{\mathcal{G}_r\}$ (note that each reactant graph can be disconnected with multiple connected components each representing a reactant). With a beam size K , for each product, G²Retro first selects the top- K most possible reaction centers from each reaction center type (BF-center, BC-center and A-center), and then selects the top- K most possible reaction centers from all the $3K$ candidates based on their corresponding scores (i.e., s^b as in Equation 8 for BF-center, s^c as in Equation 11 for BC-center, and s^a as in Equation 12 for A-center). Then G²Retro converts the product graph \mathcal{G}_p into the top- K synthon graphs $\{\mathcal{G}_{s,i}\}_{i=1}^K$ accordingly. For these synthon graphs, neighbor bond type change is predicted when necessary; atom charge change is predicted for all the atoms involved in reaction centers and their neighboring bonds \mathcal{C}_{BF} for BF-center’s. All the bond type changes and atom charge changes are predicted as those with the highest probabilities as in Equation 10 and Equation 15, respectively.

Top- N Reactant Graph Generation

Once the top- K reaction centers for each product are selected and their synthon graphs are generated, G²Retro completes the synthon graphs $\{\mathcal{G}_{s,i}\}_{i=1}^K$ into reactant graphs. During the completion, G²Retro scores each possible reactant graph and uses their final scores to select the top- N reactant graphs, and thus top- N most possible synthetic reactions, for each product. Since during synthon completion, the attachment substructure type prediction (Equation 20) gives a distribution of all possible attachment substructures; by using top possible substructures, each synthon and its intermediate graphs can be extended to multiple different intermediate graphs, leading to exponentially many reactant graphs. The intermediate graphs are denoted as $\{\mathcal{G}_{ij}^{*(t)}\}_{i=1}^K$, where $\mathcal{G}_{ij}^{*(t)}$ is for the j -th possible intermediate graph of the i -th synthon graph $\mathcal{G}_{s,i}$ at step t . However, to fully generate all the possible completed reactant graphs, excessive computation is demanded. Instead, G²Retro applies a greedy beam search strategy (algorithm A6 in Supplementary Section S2) to only explore the most possible top reactant graph completion paths.

In the beam search strategy, G²Retro scores each intermediate graph $\mathcal{G}_{ij}^{*(t)}$ using a score $s_{ij}^{(t)}$, which is calculated as the sum over all the log-likelihoods of all the predictions along the completion path from \mathcal{G}_s up to $\mathcal{G}_{ij}^{*(t)}$; $s_{ij}^{(0)}$ is initialized as the sum of the log-likelihoods of all the predictions from \mathcal{G}_p to \mathcal{G}_s . At each step t ($t \leq 30$), each intermediate graph $\mathcal{G}_{ij}^{*(t)}$ is extended to at most $N+1$ intermediate graph candidates. These $N+1$ candidates include the one that is predicted to stop at the atom that new substructures could be attached to (i.e., as $a^{(t)}$ in Equation 18; this intermediate graph could be further completed at other atoms) in this step, and at most N candidates with the top- N predicted substructures attached (Equation 20). Among all the candidates generated from all the intermediate graphs at step t , the top- N scored ones will be further forwarded into the next completion step $t+1$. In case some of the top- N graphs are fully completed, the remaining will go through the next steps. This process will be ended until the number of all the completed reactant graphs at different steps reaches or goes above N . Then, among all the incompleted graphs at the last step, the intermediate graphs with log-likelihood values higher than the N -th largest score in all the completed ones will continue to complete as above. The entire process will end until no more intermediate graphs are qualified to further completion. Among all the completed graphs, the top- N graphs are selected as the generated reactants.

Data Availability

The data used in this manuscript are available publicly at <https://github.com/ninglab/G2Retro>.

Code Availability

The code is available at no charge to academic institutions, non-profit research institutions, and governmental entities for non-commercial use.

Acknowledgements

This project was made possible, in part, by support from The Ohio State University President’s Research Excellence program (X.N., H.S.). Any opinions, findings and conclusions or recommendations expressed in this paper are those of the authors and do not necessarily reflect the views of the funding agency.

Author Contributions

X.N. conceived the research. X.N. and H.S. obtained funding for the research. Z.C. and X.N. designed the research. Z.C. and X.N. conducted the research, including data curation, formal analysis, methodology design and implementation, result analysis and visualization. Z.C. and X.N. drafted the original manuscript. O.R.A. and J.R.F. provided comments on case studies. H.S. provided comments on the original manuscript. Z.C. and X.N. conducted the manuscript editing and revision. All authors reviewed the final manuscript.

Competing Interests

The authors declare no competing interests.

References

1. Wouters, O. J., McKee, M. & Luyten, J. Estimated research and development investment needed to bring a new medicine to market, 2009-2018. *JAMA* **323**, 844 (2020).

2. Reaxys. Reaxys is a registered trademark of relx intellectual properties sa used under license. <https://www.reaxys.com>. Accessed: 2022-05-22.
3. Society, A. C. Scifinderⁿ: A cas solution. <https://scifinder-n.cas.org>. Accessed: 2022-05-22.
4. Dai, H., Li, C., Coley, C., Dai, B. & Song, L. Retrosynthesis prediction with conditional graph logic network. In Wallach, H. *et al.* (eds.) *Advances in Neural Information Processing Systems*, vol. 32 (Curran Associates, Inc., 2019).
5. Shi, C., Xu, M., Guo, H., Zhang, M. & Tang, J. A graph to graphs framework for retrosynthesis prediction. In III, H. D. & Singh, A. (eds.) *Proceedings of the 37th International Conference on Machine Learning*, vol. 119 of *Proceedings of Machine Learning Research*, 8818–8827 (PMLR, 2020).
6. Sun, R., Dai, H., Li, L., Kearnes, S. & Dai, B. Towards understanding retrosynthesis by energy-based models. In Beygelzimer, A., Dauphin, Y., Liang, P. & Vaughan, J. W. (eds.) *Advances in Neural Information Processing Systems* (2021).
7. Somnath, V. R., Bunne, C., Coley, C. W., Krause, A. & Barzilay, R. Learning graph models for retrosynthesis prediction. In Beygelzimer, A., Dauphin, Y., Liang, P. & Vaughan, J. W. (eds.) *Advances in Neural Information Processing Systems* (2021).
8. Vaswani, A. *et al.* Attention is all you need. In Guyon, I. *et al.* (eds.) *Advances in Neural Information Processing Systems*, vol. 30 (Curran Associates, Inc., 2017).
9. Kipf, T. N. & Welling, M. Semi-supervised classification with graph convolutional networks. In *5th International Conference on Learning Representations, ICLR 2017, Toulon, France, April 24–26, 2017, Conference Track Proceedings* (OpenReview.net, 2017). URL <https://openreview.net/forum?id=SJU4ayYgl>.
10. Kingma, D. P. & Welling, M. Auto-encoding variational bayes. In Bengio, Y. & LeCun, Y. (eds.) *2nd International Conference on Learning Representations, ICLR 2014, Banff, AB, Canada, April 14–16, 2014, Conference Track Proceedings* (2014). URL <http://arxiv.org/abs/1312.6114>.
11. Segler, M. H. S., Preuss, M. & Waller, M. P. Planning chemical syntheses with deep neural networks and symbolic AI. *Nature* **555**, 604–610 (2018).
12. Yan, C. *et al.* Retroxpert: Decompose retrosynthesis prediction like a chemist. In Larochelle, H., Ranzato, M., Hadsell, R., Balcan, M. F. & Lin, H. (eds.) *Advances in Neural Information Processing Systems*, vol. 33, 11248–11258 (Curran Associates, Inc., 2020).
13. Zheng, S., Rao, J., Zhang, Z., Xu, J. & Yang, Y. Predicting retrosynthetic reactions using self-corrected transformer neural networks. *Journal of Chemical Information and Modeling* **60**, 47–55 (2019).
14. Chen, B., Shen, T., Jaakkola, T. S. & Barzilay, R. Learning to make generalizable and diverse predictions for retrosynthesis 1910.09688v1.
15. Kim, E., Lee, D., Kwon, Y., Park, M. S. & Choi, Y.-S. Valid, plausible, and diverse retrosynthesis using tied two-way transformers with latent variables. *Journal of Chemical Information and Modeling* **61**, 123–133 (2021).
16. Szymkuć, S. *et al.* Computer-assisted synthetic planning: The end of the beginning. *Angewandte Chemie International Edition* **55**, 5904–5937 (2016).
17. Coley, C. W., Rogers, L., Green, W. H. & Jensen, K. F. Computer-assisted retrosynthesis based on molecular similarity. *ACS Central Science* **3**, 1237–1245 (2017).
18. Segler, M. H. S. & Waller, M. P. Neural-symbolic machine learning for retrosynthesis and reaction prediction. *Chemistry - A European Journal* **23**, 5966–5971 (2017).
19. Seidl, P. *et al.* Improving few- and zero-shot reaction template prediction using modern hopfield networks. *Journal of Chemical Information and Modeling* **62**, 2111–2120 (2022).
20. Chen, S. & Jung, Y. Deep retrosynthetic reaction prediction using local reactivity and global attention. *JACS Au* **1**, 1612–1620 (2021).
21. Mao, K. *et al.* Molecular graph enhanced transformer for retrosynthesis prediction. *Neurocomputing* **457**, 193–202 (2021).
22. Irwin, R., Dimitriadis, S., He, J. & Bjerrum, E. J. Chemformer: a pre-trained transformer for computational chemistry. *Machine Learning: Science and Technology* **3**, 015022 (2022).
23. Tu, Z. & Coley, C. W. Permutation invariant graph-to-sequence model for template-free retrosynthesis and reaction prediction (2021). 2110.09681.
24. Tetko, I. V., Karpov, P., Deursen, R. V. & Godin, G. State-of-the-art augmented NLP transformer models for direct and single-step retrosynthesis. *Nature Communications* **11** (2020).
25. Wan, Y., Liao, B., Hsieh, C.-Y. & Zhang, S. Retroformer: Pushing the limits of interpretable end-to-end retrosynthesis transformer 2201.12475v1.
26. Wang, X. *et al.* RetroPrime: A diverse, plausible and transformer-based method for single-step retrosynthesis predictions. *Chemical Engineering Journal* **420**, 129845 (2021).
27. Sacha, M. *et al.* Molecule edit graph attention network: Modeling chemical reactions as sequences of graph edits. *Journal of Chemical Information and Modeling* **61**, 3273–3284 (2021).
28. Corey, E. J. General methods for the construction of complex molecules. *Pure and Applied Chemistry* **14**, 19–38 (1967).
29. Lowe, D. M. Extraction of chemical structures and reactions from the literature (2012).
30. Schneider, N., Stiefl, N. & Landrum, G. A. What’s what: The (nearly) definitive guide to reaction role assignment. *Journal of Chemical Information and Modeling* **56**, 2336–2346 (2016).
31. Seo, S.-W. *et al.* GTA: Graph truncated attention for retrosynthesis. *Proceedings of the AAAI Conference on Artificial Intelligence* **35**, 531–539 (2021).
32. Brown, D. G. & Bostrom, J. Analysis of past and present synthetic methodologies on medicinal chemistry: Where have all the new reactions gone? *Journal of Medicinal Chemistry* **59**, 4443–4458 (2015).
33. Vijayakumar, A. K. *et al.* Diverse beam search: Decoding diverse solutions from neural sequence models 1610.02424v2.
34. Miyaura, N. & Suzuki, A. Palladium-catalyzed cross-coupling reactions of organoboron compounds. *Chemical Reviews* **95**, 2457–2483 (1995).
35. LeBlond, C. R., Andrews, A. T., Sun, Y. & Sowa, J. R. Activation of aryl chlorides for suzuki cross-coupling by ligandless, heterogeneous palladium. *Organic Letters* **3**, 1555–1557 (2001).
36. Yin & Liebscher, J. Carbon-carbon coupling reactions catalyzed by heterogeneous palladium catalysts. *Chemical Reviews* **107**, 133–173 (2006).
37. Fanta, P. E. The ullmann synthesis of biaryls. *Synthesis* **1974**, 9–21 (1974).

38. Stille, J. K. The palladium-catalyzed cross-coupling reactions of organotin reagents with organic electrophiles[new synthetic methods(58)]. *Angewandte Chemie International Edition in English* **25**, 508–524 (1986).
39. Tamao, K., Sumitani, K. & Kumada, M. Selective carbon-carbon bond formation by cross-coupling of grignard reagents with organic halides. catalysis by nickel-phosphine complexes. *Journal of the American Chemical Society* **94**, 4374–4376 (1972).
40. Yan, C. *et al.* Retroxpert. <https://github.com/uta-smile/RetroXpert> (2021).
41. Somnath, V. R. (2021). <https://github.com/uta-smile/RetroXpert/issues/15#issuecomment-864845942> Accessed: 2022-06-01.
42. Jin, W., Coley, C., Barzilay, R. & Jaakkola, T. Predicting organic reaction outcomes with weisfeiler-lehman network. In Guyon, I. *et al.* (eds.) *Advances in Neural Information Processing Systems*, vol. 30 (Curran Associates, Inc., 2017).
43. Bradshaw, J., Kusner, M. J., Paige, B., Segler, M. H. S. & Hernández-Lobato, J. M. A generative model for electron paths. In *International Conference on Learning Representations* (2019).
44. Chen, Z., Min, M. R., Parthasarathy, S. & Ning, X. A deep generative model for molecule optimization via one fragment modification. *Nature Machine Intelligence* **3**, 1040–1049 (2021).
45. Jin, W., Barzilay, D. & Jaakkola, T. Hierarchical generation of molecular graphs using structural motifs. In III, H. D. & Singh, A. (eds.) *Proceedings of the 37th International Conference on Machine Learning*, vol. 119 of *Proceedings of Machine Learning Research*, 4839–4848 (PMLR, 2020).
46. Degen, J., Wegscheid-Gerlach, C., Zaliani, A. & Rarey, M. On the art of compiling and using ‘drug-like’ chemical fragment spaces. *ChemMedChem* **3**, 1503–1507 (2008).

G²Retro: Two-Step Graph Generative Models for Retrosynthesis Prediction (Supplementary Information)

S1 Parameters for Reproducibility

We tuned the hyper-parameters of the reaction center identification module and the synthon completion module for G²Retro and G²Retro-B with the grid-search algorithm. We presented the parameter space in Table S1. We determined the optimal hyper-parameters of the two modules for G²Retro and G²Retro-B according to the corresponding top-1 accuracy over the validation molecules.

Table S1 | Hyper-parameter space for G²Retro and G²Retro-B

Hyper-parameters	Values
hidden layer dimension	{128, 256, 512}
# iterations of GMPN	{5, 7, 10}
# iterations of FMPN in G ² Retro-B	{3, 5, 7}

In the reaction center identification module, when reaction types are known, the optimal hidden dimension for G²Retro and G²Retro-B is 512; the optimal iterations of GMPN for G²Retro and G²Retro-B are 7 and 10, respectively; the optimal iteration of FMPN for G²Retro-B is 7. When reaction types are unknown, the optimal hidden dimension for G²Retro and G²Retro-B is 512 and 256, respectively; the optimal iterations of GMPN for G²Retro and G²Retro-B are 5 and 10, respectively; the optimal iteration of FMPN for G²Retro-B is 7. G²Retro and G²Retro-B share the same synthon completion model. In the synthon completion module, when reaction types are known, the optimal hidden dimension is 512; the optimal iteration of GMPN for G²Retro is 5. When reaction types are unknown, the optimal hidden dimension is 512; the optimal iterations of GMPN is 7.

We optimized the models with batch size 256, learning rate 0.001 and learning rate decay 0.9. For the reaction center module, we trained the models for 150 epochs and checked the validation accuracy at the end of each epoch. We reduced the learning rate by 0.9 if the validation accuracy does not increase by 0.01 for 10 epochs. We saved the model with the optimal top-1 accuracy on reaction center identification over the validation dataset. For the synthon completion module, we trained the models for 100 epochs and checked the validation accuracy at the end of each epoch over 2,000 reactions that are randomly sampled from the validation set. We reduced the learning rate by 0.9 if the validation accuracy does not increase by 0.01 for 5 epochs. We saved the model with the optimal top-1 accuracy on synthon completion over the sampled subset of the validation dataset.

We implemented our models using Python-3.6.9, Pytorch-1.3.1, RDKit-2019.03.4 and NetworkX-2.3. We trained our models on a Tesla P100 GPU and a CPU with 32 GB memory on Red Hat Enterprise 7.7. The training of our reaction center identification model took 16 ~ 18 hours, while the training of our synthon completion model took 32 ~ 34 hours.

S2 Algorithms of G²Retro

Algorithm A1 describes the reactant generation process of G²Retro. Given a product, the maximum number of synthons K , the beam size N , and the maximum number of steps allowed maxSteps, G²Retro generate a ranked list of N reactants that can be used to synthesize the product. Algorithm A2 describes how G²Retro converts the product graph into top- K synthon graphs. Given a product graph \mathcal{G}_p , its corresponding BRICS graph \mathcal{G}^B and K , G²Retro predicts the top- K synthon graphs and calculates their log-likelihood scores $\{s_k\}$, using the learned molecule representations from the encoder described in Algorithm A3. Specifically, G²Retro first selects the top- K most possible reaction centers and calculates their log-likelihood scores $\{s_k, C_k\}_{k=1}^K$. Then given the product graph, the top- K reaction centers and their scores and the product molecule representation \mathbf{h}_p , G²Retro transforms the product graph into top- K synthon graphs as in Algorithm A4. Algorithm A5 describes how G²Retro completes top- K synthon graphs into top- N reactant graphs. Given the product graph \mathcal{G}_p , the top- K synthon graphs and their scores $\{s_k, \mathcal{G}_{s,k}\}_{k=1}^K$, the beam size N , and the maximum number of completion steps maxSteps, G²Retro uses a beam search strategy to complete the synthon graphs into the reactant graphs in a sequential way. Algorithm A6 describes the beam search strategy. Given the queue of intermediate molecules Q , the queue of completed reactants R , the representations of top- K synthons $\{\mathbf{h}_{s,k}\}_{k=1}^K$, the product representation \mathbf{h}_p , and the beam size N , G²Retro extends each intermediate molecule in the queue by attaching different substructures at the attachment point, and saves the completed molecules into R and the incompleted ones for the next completion step. Algorithm A7 describes how to attach new substructures to an intermediate molecule using the Attachment Continuity Prediction (AACP) and the Attachment Type Prediction (AATP).

Algorithm A1 G²Retro

Require: $M_p = (\mathcal{G}_p, \mathcal{G}_p^B)$, K , N , maxSteps▷ predict top- K synthons1: $\{s_k, \mathcal{G}_{s,k}\}_{k=1}^K = \text{G}^2\text{Retro-RCI}(\mathcal{G}_p, \mathcal{G}_p^B, K)$ ▷ predict top- N reactants2: $\{\mathcal{G}_{r,i}\}_{i=1}^N = \text{G}^2\text{Retro-SC}(\mathcal{G}_p, \{s_k, \mathcal{G}_{s,k}\}_{k=1}^K, N, \text{maxSteps})$ 3: **return** $\{\mathcal{G}_{r,i}\}_{i=1}^N$

Algorithm A2 G²Retro-RCI

Require: $\mathcal{G}_p, \mathcal{G}^B, K$

▷ learn molecule representations

1: $\{\mathbf{a}_i\}, \{\mathbf{b}_{ij}\}, \mathbf{h}_p = \text{G}^2\text{Retro-encoder}(\mathcal{G}_p, \mathcal{G}^B)$ ▷ select top- K BF-centers (Equation 8)2: $\{s^b(b_{ij})\}^K = \text{top}(K, \text{findCenter}(\text{BF-center}, \{\mathbf{b}_{ij}\}, \mathbf{h}_p))$ ▷ select top- K BC-centers (Equation 11)3: $\{s_k^c(b_{ij})\}^K = \text{top}(K, \text{findCenter}(\text{BC-center}, \{\mathbf{b}_{ij}\}, \mathbf{h}_p))$ ▷ select top- K A-centers (Equation 12)4: $\{s^a(a_i)\}^K = \text{top}(K, \text{findCenter}(\text{A-center}, \{\mathbf{a}_i\}, \mathbf{h}_p))$ ▷ select top- K centers $\{C_k\}$ and calculate their log-likelihoods $\{s_k\}$ 5: $\{s_k, C_k\}_{k=1}^K = \text{top}(K, \{s^b(b_{ij})\}^K, \{s_k^c(b_{ij})\}^K, \{s^a(a_i)\}^K)$ ▷ convert a product into K sets of synthons and update their log-likelihoods6: $\{s_k, \mathcal{G}_{s,k}\}_{k=1}^K = \text{G}^2\text{Retro-p2s-T}(\mathcal{G}_p, \{s_k, C_k\}_{k=1}^K, \mathbf{h}_p)$ 7: **return** $\{s_k, \mathcal{G}_{s,k}\}_{k=1}^K$

Algorithm A3 G²Retro-encoder

Require: $\mathcal{G}, \mathcal{G}^B$

▷ calculate atom embeddings

1: $\{\mathbf{a}_i\} = \text{GMPN}(\mathcal{G})$

▷ calculate the graph embedding (Equation 3)

2: $\mathbf{h} = \sum_{a_i \in \mathcal{G}} \mathbf{a}_i$ 3: **if** use BRICS **then**4: $\{\mathbf{n}_u\} = \text{FMPN}(\mathcal{G}^B, \{\mathbf{a}_i\})$

▷ update the embedding of each atom with its BRICS fragment embedding (Equation 6)

5: $\{\mathbf{a}_i\} = \{V(\mathbf{a}_i \oplus \mathbf{n}_u)\}$ 6: **end if**

▷ calculate bond embeddings (Equation 7)

7: $\{\mathbf{b}_{ij}\} = \text{bondEmb}(\{\mathbf{a}_i\})$ 8: **return** $\{\mathbf{a}_i\}, \{\mathbf{b}_{ij}\}, \mathbf{h}$

Algorithm A4 G²Retro-*p2s*-T

Require: $\mathcal{G}_p, \{s_k, C_k\}_{k=1}^K, \mathbf{h}_p$

```
1: for each  $s_k, C_k$  do
2:   if  $C_k$  is BF-center then
      $\triangleright$  predict bonds with induced type changes and calculate the log-likelihood  $s_{\text{BF}}$  for the predictions of  $\mathcal{C}_{\text{BF}}(C_k)$ 
3:      $\mathcal{C}_{\text{BF}}'(C_k), s_{\text{BF}} = \text{BTCP}(C_k, \mathcal{C}_{\text{BF}}(C_k), \mathbf{h}_p)$ 
      $\triangleright$  add the predicted bonds with type changes into the center
4:      $C_k = C_k \cup \mathcal{C}_{\text{BF}}'(C_k)$ 
      $\triangleright$  update the log-likelihood score
5:      $s_k = s_k + s_{\text{BF}}$ 
6:   end if
      $\triangleright$  predict atoms with charge changes for all the atoms within the center  $\mathcal{C}_{\text{A}}(C_k)$ , and calculate the log-likelihood
     score  $s_{\text{A}}$  for the predictions of  $\mathcal{C}_{\text{A}}(C_k)$ 
7:      $\mathcal{C}_{\text{A}}'(C_k), s_{\text{A}} = \text{ACP}(C_k, \mathcal{C}_{\text{A}}(C_k), \mathbf{h}_p)$ 
      $\triangleright$  update the log-likelihood score
8:      $s_k = s_k + s_{\text{A}}$ 
      $\triangleright$  transform the product graph into the synthon graph
9:      $\mathcal{G}_{s,k} = \text{transform}(\mathcal{G}_p, C_k, \mathcal{C}_{\text{A}}'(C_k))$ 
10: end for
11: return  $\{s_k, \mathcal{G}_{s,k}\}_{k=1}^K$ 
```

Algorithm A5 G²Retro-SC

Require: $\mathcal{G}_p, \{s_k, \mathcal{G}_{s,k}\}_{k=1}^K, N, \text{maxSteps}$

```
1:  $t = 0$ 
    $\triangleright$  learn molecule representations
2:  $\_, \_, \mathbf{h}_p = \text{G}^2\text{Retro-encoder}(\mathcal{G}_p)$ 
3:  $\_, \_, \{\mathbf{h}_{s,k}\}_{k=1}^K = \text{G}^2\text{Retro-encoder}(\{\mathcal{G}_{s,k}\}_{k=1}^K)$ 
    $\triangleright$  initialize a priority queue with synthons  $\{\mathcal{G}_{s,k}\}_{k=1}^K$  as elements and  $\{s_k\}_{k=1}^K$  as their priorities
4:  $Q^{(0)} = \text{priorityQueue}(\{s_k, \mathcal{G}_{s,k}\}_{k=1}^K)$ 
    $\triangleright$  initialize an empty priority queue to store complete reactants
5:  $R = \text{priorityQueue}()$ 
6: while  $!Q^{(t)}.isEmpty()$  and  $t \leq \text{maxSteps}$  do
      $\triangleright$  stop the completion when it is impossible to get reactants better than the top- $N$  reactants in  $R$ 
7:   if  $R.size() \geq N$  and  $R.\text{nthLargestPriority}(N) \geq Q^{(t)}.maxPriority()$  then
8:     break
9:   end if
      $\triangleright$  complete synthons through beam search
10:   $Q^{(t+1)}, R = \text{G}^2\text{Retro-beam-search}(Q^{(t)}, R, \{\mathbf{h}_{s,k}\}_{k=1}^K, \mathbf{h}_p, N)$ 
11:   $t = t + 1$ 
12: end while
    $\triangleright$  output top- $N$  reactants
13:  $\{\mathcal{G}_{r,i}\}_{i=1}^N = R.\text{nLargest}(N)$ 
14: return  $\{\mathcal{G}_{r,i}\}_{i=1}^N$ 
```

Algorithm A6 G²Retro-beam-search

Require: $Q, R, \{\mathbf{h}_{s,k}\}_{k=1}^K, \mathbf{h}_p, N$

```
1:  $I = Q.size()$ 
2:  $Q' = priorityQueue()$ 
3: while ! $Q.isEmpty()$  do
4:    $s_i, \mathcal{G}_i^* = Q.pop()$ 
       $\triangleright$  get the index of the synthon corresponding to  $\mathcal{G}_i^*$ 
5:    $k = \mathcal{G}_i^*.getSynthonIdx()$ 
       $\triangleright$  predict the atom attachment for  $\mathcal{G}_i^*$ 
6:    $\{s_{i,j}, \mathcal{G}'_{i,j}\}_{j=1}^{N+1} = \text{G}^2\text{Retro-AAP}(\mathcal{G}_i^*, s_i, \mathbf{h}_{s,k}, \mathbf{h}_p, N)$ 
7: end while
       $\triangleright$  select top- $N$  intermediate graph candidates
8:  $\{s_i, \mathcal{G}'_i\}_{i=1}^N = \text{top}(N, \{\{s_{i,j}, \mathcal{G}'_{i,j}\}_{j=1}^{N+1}\}_{i=1}^I)$ 
9: for each  $s_i, \mathcal{G}'_i$  do
10:   if  $\mathcal{G}'_i.isComplete()$  then
11:      $R.push(s_i, \mathcal{G}'_i)$ 
12:   else
13:      $Q'.push(s_i, \mathcal{G}'_i)$ 
14:   end if
15: end for
16: return  $Q', R$ 
```

Algorithm A7 G²Retro-AAP

Require: $\mathcal{G}^*, s, \mathbf{h}_s, \mathbf{h}_p, N$

```
 $\triangleright$  get the atom that new substructures will be attached to
1:  $a = \mathcal{G}^*.nextAttachmentPoint()$ 
 $\triangleright$  predict whether further attachment should be added to  $a$  (Equation 18)
2:  $s^o, s^{-o} = \text{AACP}(a, \mathbf{h}_s, \mathbf{h}_p)$ 
 $\triangleright$  extend  $\mathcal{G}^*$  to the candidate  $\mathcal{G}'_1$  that is predicted to stop at  $a$ 
3:  $\mathcal{G}'_1 = \text{stop}(\mathcal{G}^*, a)$ 
 $\triangleright$  update the log-likelihood value of  $\mathcal{G}'_1$ 
4:  $s'_1 = s + s^{-o}$ 
 $\triangleright$  predict the top- $N$  new substructure attachments (Equation 20)
5:  $\{z_i, s^z_i\}_{i=1}^N = \text{top}(N, \text{AATP}(a, \mathbf{h}_s, \mathbf{h}_p))$ 
 $\triangleright$  extend  $\mathcal{G}^*$  to the candidates  $\{\mathcal{G}'_i\}_{i=2}^{N+1}$  with the top- $N$  substructures
6:  $\{\mathcal{G}'_i\}_{i=2}^{N+1} = \text{attach}(\mathcal{G}^*, \{z_i\}_{i=1}^N)$ 
 $\triangleright$  update the log-likelihood values of  $\{\mathcal{G}'_i\}_{i=2}^{N+1}$ 
7:  $\{s'_i\}_{i=2}^{N+1} = \{s + s^o + s^z_i\}_{i=1}^N$ 
8: return  $\{s'_i, \mathcal{G}'_i\}_{i=1}^{N+1}$ 
```

S3 Substructures used to complete synthons

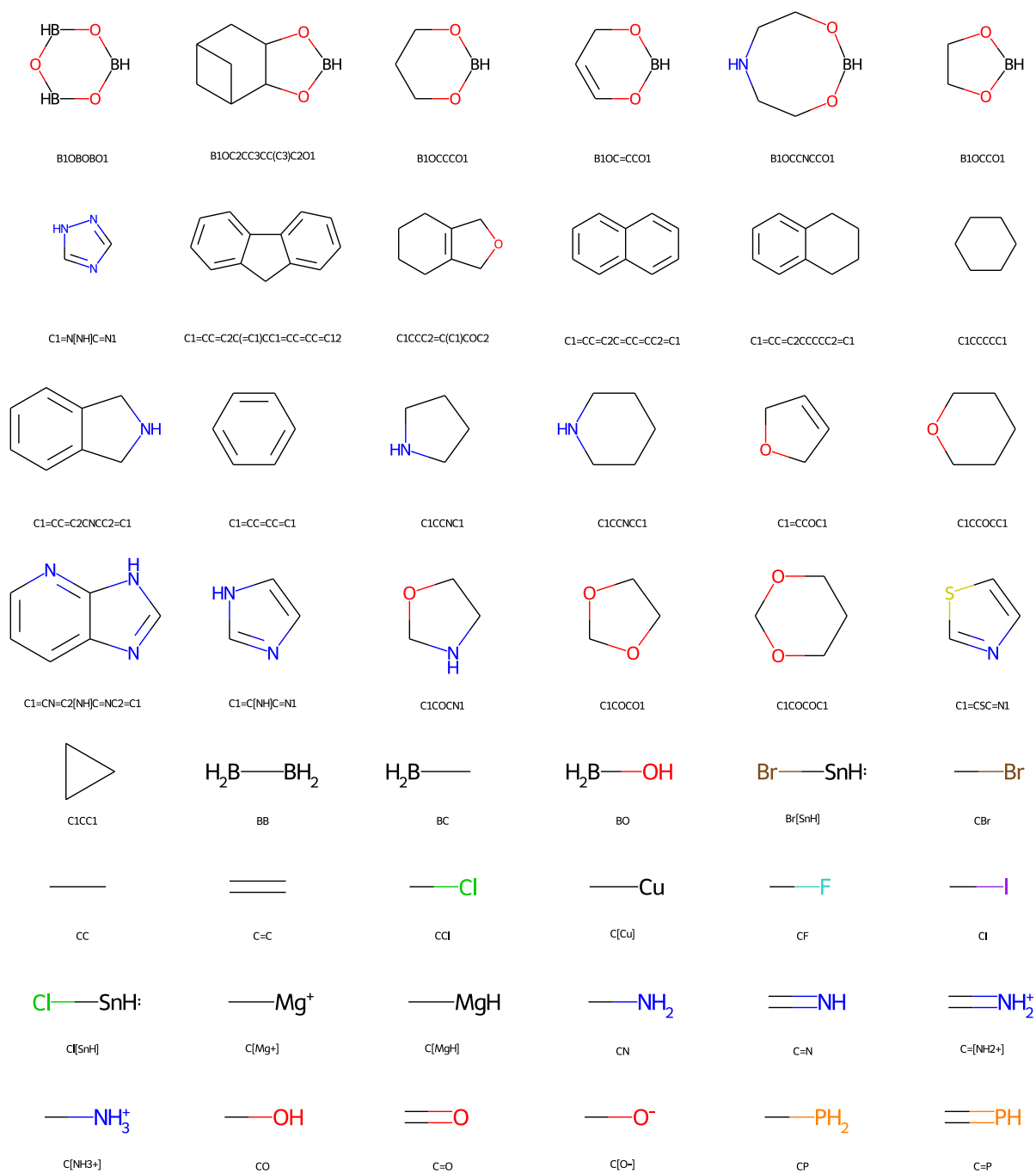


Fig. S1 | 83 substructures that G²Retro uses to complete synthons

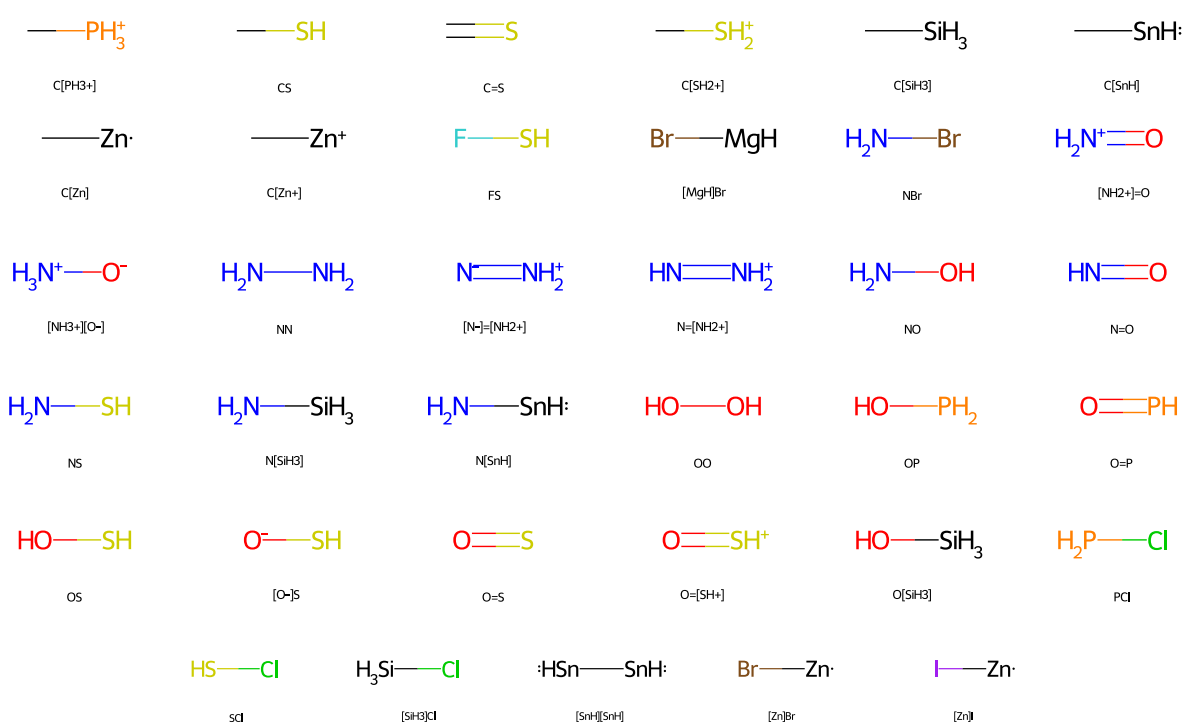


Fig. S1 | 83 substructures that G²Retro uses to complete synthons